



HHS Public Access

Author manuscript

Nat Genet. Author manuscript; available in PMC 2022 November 12.

Published in final edited form as:

Nat Genet. 2022 May ; 54(5): 560–572. doi:10.1038/s41588-022-01058-3.

Users may view, print, copy, and download text and data-mine the content in such documents, for the purposes of academic research, subject always to the full Conditions of use: <https://www.springernature.com/gp/open-research/policies/accepted-manuscript-terms>

‡ mahajan.anubha@gene.com; mccarthy.mark@gene.com; andrew.morris-5@manchester.ac.uk

*These authors contributed equally to this work.

†These authors supervised this work.

AUTHOR CONTRIBUTIONS

DIAMANTE Consortium co-ordination: A. Mahajan, M.I.M., A.P.M. *Manuscript preparation*: A. Mahajan, C.N.S., W. Zhang, M.C.Y.N., L.E.P., H.K., G.Z.Y., S. Rüeger, L.S., A.L.G., M.B., J.I.R., M.I.M., A.P.M. *Co-ordination of ancestry-specific GWAS collections*: A. Mahajan, C.N.S., W. Zhang, M.C.Y.N., L.E.P., D.W.B., J.E.B., J.C.C., X.S., M.B. *Central analysis group*: A. Mahajan, C.N.S., W. Zhang, M.C.Y.N., L.E.P., H.K., Y.J.K., M. Horikoshi, J.M.M., D.T., S. Moon, S.-H.K., N.R.R., N.W.R., M. Loh, B.-J.K., J. Flanagan, J.B.M., K.L.M., J.E.B., J.C.C., X.S., M.B., J.I.R., M.I.M., A.P.M. *PROX1 functional analyses*: G.Z.Y., F.A., J.M.T., A.L.G. *GRS analyses in FinnGen*: S. Rüeger, P.d.B.P. *Selection analyses*: L.S., S.R.M. *Single cell chromatin accessibility data*: J. Chiou, D.G., S.P., M. Sander, K.J.G. *Islet promoter HiC data generation*: I.M.-E., J. Ferrer. *Study-level primary analyses*: A. Mahajan, C.N.S., W. Zhang, M.C.Y.N., L.E.P., Y.J.K., M. Horikoshi, J.M.M., D.T., S. Moon, S.-H.K., K. Lin, F.B., M.H.P., F.T., J.N., X.G., A. Lamri, M.N., R.A.S., J.-J.L., A.H.-G., M. Graff, J.-F.C., E.J.P., J.Y., L.F.B., Y.T., Y.H., V.S., J.P.C., M.K., N.G., E.M.S., I.P., T.S., M.W., C. Sarnowski, C.G., D.N., S. Trompet, J. Long, M. Sun, L.T., W.-M.C., M. Ahmad, R.N., V.J.Y.L., C.H.T.T., Y.Y.J., C.-H.C., L.M.R., C. Lecoeur, B.P.P., A.N., L.R.Y., G.C., R.A.J., S. Tajuddin, E.K.K., P.A., A.H.X., H.S.C., B.E.C., J.Tan, X.S., A.P.M. *Study-level phenotyping, genotyping and additional analyses*: L.S.A., A.A., C.A.A.-S., M. Akiyama, S.S.A., A.B., Z.B., J.B.-J., J.A.B., C.M.B., T.B., M. Canouil, J.C.N.C., L.-C.C., M.L.C., J. Chen, S.-C.K., Y.-T.C., Z.C., C.C., L.-M.C., M. Cushman, S.K.D., H.J.d.S., G.D., L.D., A.P.D., S.D., Q.D., K.-U.E., L.S.E., D.S.E., M.K.E., K.F., J.S.F., I.F., M.F., O.H.F., T.M.F., B.I.F., C.F., P.G., H.C.G., V.G., C.G.-V., M.E.G.-V., M.O.G., P.G.-L., M. Gross, Y.G., S. Hackinger, S. Han, A.T.H., C.H., A.-G.H., W. Hsueh, M. Huang, W. Huang, Y.-J.H., M.Y.H., C.-M.H., S.I., M.A.I., M. Ingelsson, M.T.I., M. Isono, H.-M.J., F.J., G.J., J.B.J., M.E.J., T.J., Y.K., F.R.K., A. Kasturiratne, T. Katsuya, V.K., T. Kawaguchi, J.M.K., A.N.K., C.-C.K., M.G.K., K.K., J. Kriebel, F.K., J. Kuusisto, K. Läll, L.A.L., M.-S.L., N.R.L., A. Leong, L. Li, Y. Li, R.L.-G., S. Ligthart, C.M.L., A. Linneberg, C.-T.L., J. Liu, A.E.L., T.L., J. Luan, A.O.L., X.L., J. Lv, V.L., V.M., K.R.M., T.M., A. Metspalu, A.D.M., G.N.N., J.L.N., M.A.N., U.N., S.S.N., I.N., Y.O., L.O., S.R.P., M.A. Pereira, A.P., F.J.P., B.P., G. Prasad, L.J.R.-T., A.P.R., M.R., R.R., K.R., C. Sabanayagam, K. Sandow, N.S., S.S., C. Schurmann, M. Shahriar, J.S., D.M.S., D. Shriner, J.A.S., W.Y.S., A.S., A.M.S., K. Strauch, K. Suzuki, A.T., K.D.T., B. Thorand, G.T., U.T., B. Tomlinson, F.-J.T., J. Tuomilehto, T.T.-L., M.S.U., A.V.-S., R.M.v.D., J.B.v.K., R.V., M.V., N.W.-R., E.W., E.A.W., A.R.W., K.W.v.D., D.R.W., Y.-B.X., C.S.Y., K. Yamamoto, T.Y., L.Y., K. Yoon, C.Y., J.-M.Y., S.Y., L.Z., W. Zheng. *Study-level principal investigator*: L.J.R., M. Igase, E. Ipp, S. Redline, Y.S.C., L. Lind, M.A. Province, C.L.H., P.A.P., E. Ingelsson, A.B.Z., B.M.P., Y.-X.W., C.N.R., D.M.B., F.M., Y. Liu, E.Z., M.Y., S.S.R., C.K., J.S.P., J.C.E., Y.-D.I.C., P.F., J.G.W., W.H.H.S., S.L.R.K., J.-Y.W., M.G.H., R.C.W.M., T.-Y.W., L.G., D.O.M.-K., G.R.C., F.S.C., D.B., G. Pare, M.M.S., H.A., A.A.M., X.-O.S., K.-S.P., J.W.J., M. Cruz, R.M.-C., H.G., C.-Y.C., E.P.B., A.D., E.-S.T., J.D., N.K., M. Laakso, A. Köttgen, W.-P.K., C.N.A.P., S. Liu, G.A., J.S.K., R.J.F.L., K.E.N., C.A.H., J.C.F., D. Saleheen, T.H., O.P., R.M., C. Langenberg, N.J.W., S. Maeda, T. Kadowaki, J. Lee, I.Y.M., R.G.W., K. Stefansson, J.B.M., K.L.M., D.W.B., J.C.C., M.B., J.I.R., M.I.M., A.P.M.

COMPETING INTERESTS

A. Mahajan is now an employee of Genentech and a holder of Roche stock. R.A.S. is now an employee of GlaxoSmithKline. V.S. is now an employee of deCODE genetics/Amgen Inc. L.S.E. is now an employee of Bristol Myers Squibb. J.S.F. has consulted for Shionogi Inc. T.M.F. has consulted for Sanofi, Boehringer Ingelheim and received funding from GSK. H.C.G. holds the McMaster-Sanofi Population Health Institute Chair in Diabetes Research and Care; reports research grants from Eli Lilly, AstraZeneca, Merck, Novo Nordisk and Sanofi; honoraria for speaking from AstraZeneca, Boehringer Ingelheim, Eli Lilly, Novo Nordisk, DKSH, Zuellig, Roche, and Sanofi; and consulting fees from Abbott, AstraZeneca, Boehringer Ingelheim, Eli Lilly, Merck, Novo Nordisk, Pfizer, Sanofi, Kowa and Hanmi. M. Ingelsson is a paid consultant to BioArctic AB. R.L.-G. is a part-time consultant of Metabolon Inc. A.E.L. is now an employee of Regeneron Genetics Center, LLC and holds shares in Regeneron Pharmaceuticals. M.A.N. currently serves on the scientific advisory board for Clover Therapeutics and is an advisor to Neuron23 Inc. S.R.P. has received grant funding from Bayer Pharmaceuticals, Philips Respironics and Respicardia. N.S. has consulted for or been on speakers bureau for Abbott, Amgen, Astrazeneca, Boehringer Ingelheim, Eli Lilly, Hanmi, Novartis, Novo Nordisk, Sanofi and Pfizer and has received grant funding from Astrazeneca, Boehringer Ingelheim, Novartis and Roche Diagnostics. A.M.S. receives funding from Seven Bridges Genomics to develop tools for the NHLBI BioData Catalyst consortium. G.T. is an employee of deCODE genetics/Amgen Inc. U.T. is an employee of deCODE genetics/Amgen Inc. E. Ingelsson is now an employee of GlaxoSmithKline. B.M.P. serves on the Steering Committee of the Yale Open Data Access Project funded by Johnson & Johnson. R.C.W.M. reports research funding from AstraZeneca, Bayer, Novo Nordisk, Pfizer, Tricida Inc. and Sanofi, and has consulted for or received speakers fees from AstraZeneca, Bayer, Boehringer Ingelheim, all of which have been donated to the Chinese University of Hong Kong to support diabetes research. D.O.M.-K. is a part-time clinical research consultant for Metabolon Inc. S. Liu reports consulting payments and honoraria or promises of the same for scientific presentations or reviews at numerous venues, including but not limited to Barilla, by-Health Inc, AUSA Pharmed Co.LTD, Fred Hutchinson Cancer Center, Harvard University, University of Buffalo, Guangdong General Hospital and Academy of Medical Sciences, Consulting member for Novo Nordisk, Inc; member of the Data Safety and Monitoring Board for a trial of pulmonary hypertension in diabetes patients at Massachusetts General Hospital; receives royalties from UpToDate; receives an honorarium from the American Society for Nutrition for his duties as Associate Editor. K. Stefansson is an employee of deCODE genetics/Amgen Inc. K.J.G. does consulting for Genentech and holds stock in Vertex Pharmaceuticals. A.L.G.'s spouse is an employee of Genentech and holds stock options in Roche. M.I.M. has served on advisory panels for Pfizer, NovoNordisk and Zoe Global, has received honoraria from Merck, Pfizer, Novo Nordisk and Eli Lilly, and research funding from Abbvie, Astra Zeneca, Boehringer Ingelheim, Eli Lilly,

Multi-ancestry genetic study of type 2 diabetes highlights the power of diverse populations for discovery and translation

A full list of authors and affiliations appears at the end of the article.

Abstract

We assembled an ancestrally diverse collection of genome-wide association studies (GWAS) of type 2 diabetes (T2D) in 180,834 cases and 1,159,055 controls (48.9% non-European descent) through the DIAMANTE (DIAbetes Meta-ANalysis of Trans-Ethnic association studies) Consortium. Multi-ancestry GWAS meta-analysis identified 237 loci attaining stringent genome-wide significance ($P < 5 \times 10^{-9}$), which were delineated to 338 distinct association signals. Fine-mapping of these signals was enhanced by the increased sample size and expanded population diversity of the multi-ancestry meta-analysis, which localized 54.4% of T2D associations to a single variant with >50% posterior probability. This improved fine-mapping enabled systematic assessment of candidate causal genes and molecular mechanisms through which T2D associations are mediated, laying the foundations for functional investigations. Multi-ancestry genetic risk scores enhanced transferability of T2D prediction across diverse populations. Our study provides a step towards more effective clinical translation of T2D GWAS to improve global health for all, irrespective of genetic background.

The global prevalence of type 2 diabetes (T2D) has quadrupled over the last 30 years¹, affecting approximately 392 million individuals in 2015². Despite this worldwide impact, the largest T2D genome-wide association studies (GWAS) have predominantly featured populations of European ancestry³⁻⁶, compromising prospects for clinical translation. Failure to detect causal variants that contribute to disease risk outside European ancestry populations limits progress towards a full understanding of disease biology and constrains opportunities for development of therapeutics⁷. Implementation of personalized approaches to disease management depends on accurate prediction of individual risk, irrespective of ancestry. However, genetic risk scores (GRS) derived from European ancestry GWAS provide unreliable prediction when deployed in other population groups, in part reflecting differences in effect sizes, allele frequencies and patterns of linkage disequilibrium (LD)⁸.

To address the impact of this population bias, recent T2D GWAS have included individuals of non-European ancestry⁹⁻¹¹. The DIAMANTE (DIAbetes Meta-ANalysis of Trans-Ethnic association studies) Consortium was established to assemble T2D GWAS across diverse ancestry groups. Analyses of the European and East Asian ancestry components of DIAMANTE have previously been reported^{6,10}. Here, we describe the results of our multi-

Janssen, Merck, NovoNordisk, Pfizer, Roche, Sanofi Aventis, Servier, and Takeda; is now an employee of Genentech and a holder of Roche stock. The remaining authors declare no competing interests.

The views expressed in this article are those of the authors and do not necessarily represent those of: the NHS, the NIHR, or the UK Department of Health; the National Heart, Lung, and Blood Institute, the National Institutes of Health, or the US Department of Health and Human Services.

ancestry meta-analysis, which expands on these published components to a total of 180,834 T2D cases and 1,159,055 controls, with 20.5% of the effective sample size ascertained from African, Hispanic, and South Asian ancestry groups. With these data, we demonstrate the value of analyses conducted in diverse populations to understand how T2D-associated variants impact downstream molecular and biological processes underlying the disease, and advance clinical translation of GWAS findings for all, irrespective of genetic background.

RESULTS

Study overview.

We accumulated association summary statistics from 122 GWAS in 180,834 T2D cases and 1,159,055 controls (effective sample size 492,191) across five ancestry groups (Supplementary Tables 1-3). We use the term “ancestry group” to refer to individuals with similar genetic background: European ancestry (51.1% of the total effective sample size); East Asian ancestry (28.4%); South Asian ancestry (8.3%); African ancestry, including recently admixed African American populations (6.6%); and Hispanic individuals with recent admixture of American, African, and European ancestry (5.6%). Each ancestry-specific GWAS was imputed to reference panels from the 1000 Genomes Project^{12,13}, Haplotype Reference Consortium¹⁴, or population-specific whole-genome sequence data. Subsequent association analyses were adjusted for population structure and relatedness (Supplementary Table 4). We considered 19,829,461 bi-allelic autosomal single nucleotide variants (SNVs) that overlapped reference panels with minor allele frequency (MAF) > 0.5% in at least one of the five ancestry groups (Extended Data Fig. 1 and Methods).

Robust discovery of multi-ancestry T2D associations.

We aggregated association summary statistics via multi-ancestry meta-regression, implemented in MR-MEGA¹⁵, which models allelic effect heterogeneity correlated with genetic ancestry. We included three axes of genetic variation as covariates that separated GWAS from the five major ancestry groups (Extended Data Fig. 2 and Methods). We identified 277 loci associated with T2D at the conventional genome-wide significance threshold of $P < 5 \times 10^{-8}$ (Extended Data Fig. 3 and Supplementary Table 5). By accounting for ancestry-correlated allelic effect heterogeneity in the multi-ancestry meta-regression, we observed lower genomic control inflation ($\lambda_{GC} = 1.05$) than when using either fixed- or random-effects meta-analysis ($\lambda_{GC} = 1.25$ under both models), and stronger signals of association at lead SNVs at most loci (Extended Data Fig. 4). Of the 277 loci, 11 have not previously been reported in recently published T2D GWAS meta-analyses^{6,10,11} that account for 78.6% of the total effective sample size of this multi-ancestry meta-regression (Extended Data Fig. 3 and Supplementary Note). Of the 100 and 193 loci attaining genome-wide significance ($P < 5 \times 10^{-8}$) in East Asian and European ancestry-specific meta-analyses, respectively, lead SNVs at 94 (94.0%) and 164 (85.0%) demonstrated stronger evidence for association (smaller P -value) in the multi-ancestry meta-regression (Extended Data Fig. 5 and Supplementary Note). These results demonstrate the power of multi-ancestry meta-analyses for locus discovery afforded by increased sample size, but also emphasize the importance of complementary ancestry-specific GWAS for identification of associations that are not shared across diverse populations.

The conventional genome-wide significance threshold does not allow for different patterns of LD across diverse populations in multi-ancestry meta-analysis. We therefore derived a multi-ancestry genome-wide significance threshold of $P < 5 \times 10^{-9}$ by estimating the effective number of independent SNVs across the five ancestry groups using haplotypes from the 1000 Genomes Project reference panel¹³ (Methods). Of the 277 loci reported in this multi-ancestry meta-regression, 237 attained the more stringent significance threshold, which we considered for downstream analyses. Through approximate conditional analyses, conducted using ancestry-matched LD reference panels for each GWAS, we partitioned associations at the 237 loci into 338 distinct signals that were each represented by an index SNV at the same multi-ancestry genome-wide significance threshold (Methods, Supplementary Tables 6-8, and Supplementary Note). Allelic effect estimates for distinct association signals from approximate conditional analyses undertaken in admixed ancestry groups were robust to the choice of reference panel (Supplementary Note).

Allelic-effect heterogeneity across ancestry groups.

Allelic-effect heterogeneity between ancestry groups can occur for several reasons, including differences in LD with causal variants or interactions with environment or polygenic background across diverse populations. An advantage of the multi-ancestry meta-regression model is that heterogeneity can be partitioned into two components. The first captures heterogeneity that is correlated with genetic ancestry (i.e. can be explained by the three axes of genetic variation). The second reflects residual heterogeneity due to differences in geographical location (for example different environmental exposures) and study design (for example different phenotype definition, case-control ascertainment, or covariate adjustments between GWAS). We observed 136 (40.2%) distinct T2D associations with nominal evidence ($P_{HET} < 0.05$) of ancestry-correlated heterogeneity compared to 16.9 expected by chance (binomial test $P < 2.2 \times 10^{-16}$). In contrast, there was nominal evidence of residual heterogeneity at just 27 (8.0%) T2D association signals (binomial test $P = 0.0037$), suggesting that differences in allelic effect size between GWAS are more likely due to factors related to genetic ancestry than to geography and/or study design (Supplementary Note).

Population diversity improves fine-mapping resolution.

We sought to quantify the improvement in fine-mapping resolution offered by increased sample size and population diversity in the multi-ancestry meta-regression. For each of the 338 distinct signals, we first derived multi-ancestry and European ancestry-specific credible sets of variants that account for 99% of the posterior probability (π) of driving the T2D association under a uniform prior model of causality (Methods). Multi-ancestry meta-regression substantially reduced the median 99% credible set size from 35 variants (spanning 112 kb) to 10 variants (spanning 26 kb), and increased the median posterior probability ascribed to the index SNV from 24.3% to 42.0%. The 99% credible sets for 266 (78.7%) distinct T2D associations were smaller in the multi-ancestry meta-regression than in the European ancestry-specific meta-analysis, while a further 26 (7.7%) signals were resolved to a single SNV in both (Fig. 1, Supplementary Table 9, and Supplementary Note). Causal variant localization was also more precise in the multi-ancestry meta-regression than a meta-analysis of GWAS of European and East Asian ancestry, which together account for

79.5% of the total effective sample size, highlighting the important contribution of the most under-represented ancestry groups (African, Hispanic, and South Asian) to fine-mapping resolution (Fig. 1 and Supplementary Note).

We next attempted to understand the relative contributions of population diversity and sample size to these improvements in fine-mapping resolution at the 266 distinct T2D associations that were more precisely localized after the multi-ancestry meta-regression. We down-sampled studies contributing to the multi-ancestry meta-regression to approximate the effective sample size of the European ancestry-specific meta-analysis, while maintaining the distribution of population diversity (Methods and Supplementary Table 10). The associations were better resolved in the down-sampled multi-ancestry meta-regression at 137 signals (51.5%), compared with 119 signals (44.7%) in the European ancestry-specific meta-analysis (Fig. 1 and Supplementary Table 11). These results highlight the value of diverse populations for causal variant localization in multi-ancestry meta-analysis, emphasizing the importance of increased sample size and differences in LD structure and allele frequency distribution between ancestry groups that has also been reported for other complex human traits¹⁶.

Multi-ancestry fine-mapping to single variant resolution.

Previous T2D GWAS have demonstrated improved localization of causal variants through integration of fine-mapping data with genomic annotation^{6,17}. By mapping SNVs to three categories of functional and regulatory annotation, with an emphasis on diabetes-relevant tissues¹⁸, we observed significant joint enrichment ($P < 0.00023$, Bonferroni correction for 220 annotations) for T2D associations mapping to protein coding exons, binding sites for NKX2.2, FOXA2, EZH2, and PDX1, and four chromatin states in pancreatic islets that mark active enhancers, active promoters, and transcribed regions (Methods, Extended Data Fig. 6 and Supplementary Table 12). We used the enriched annotations to derive a prior model for causality, and redefined 99% credible sets of variants for each distinct signal (Methods and Supplementary Table 13). Annotation-informed fine-mapping reduced the size of the 99% credible set, compared to the uniform prior, at 144 (42.6%) distinct association signals (Extended Data Fig. 7), and decreased the median from 10 variants (spanning 26 kb) to 8 variants (spanning 23 kb). For 184 (54.4%) signals, a single SNV accounted for >50% of the posterior probability of the T2D association (Supplementary Table 14). At 124 (36.7%) signals, >80% of the posterior probability could be attributed to a single SNV.

Missense variants implicate candidate causal genes.

After annotation-informed multi-ancestry fine-mapping, 19 of the 184 SNVs accounting for >50% of the posterior probability of the T2D association were missense variants (Supplementary Table 15). Two of these implicate novel candidate causal genes for the disease: *MYO5C* p.Glu1075Lys (rs3825801, $P = 3.8 \times 10^{-11}$, $\pi = 69.2\%$) at the *MYO5C* locus, and *ACVR1C* p.Ile482Val (rs7594480, $P = 4.0 \times 10^{-12}$, $\pi = 95.2\%$) at the *CYTIP* locus. *ACVR1C* encodes ALK7, a transforming growth factor- β receptor, overexpression of which induces growth inhibition and apoptosis of pancreatic β -cells¹⁹; *ACVR1C* p.Ile482Val has been previously associated with body fat distribution²⁰. The multi-ancestry meta-regression also highlighted examples of previously reported associations that were

better resolved by fine-mapping across diverse populations, including *SLC16A11*, *KCNJ11-ABCC8*, and *ZFAND3-KCNK16-GLP1R* (Supplementary Note).

Multi-omics integration highlights candidate effector genes.

We next sought to take advantage of the improved fine-mapping resolution offered by the multi-ancestry meta-regression to extend insights into candidate effector genes, tissue specificity, and mechanisms through which regulatory variants at non-coding T2D association signals impact disease risk. We integrated annotation-informed fine-mapping data with molecular quantitative trait loci (QTLs), in *cis*, for: (i) circulating plasma proteins (pQTLs)²¹; and (ii) gene expression (eQTLs) in diverse tissues, including pancreatic islets, subcutaneous and visceral adipose, liver, skeletal muscle, and hypothalamus^{22,23} (Methods). Bayesian colocalization²⁴ of each pair of distinct T2D associations and molecular QTLs identified 97 candidate effector genes at 72 signals with posterior probability $\pi_{\text{COLOC}} > 80\%$ (Supplementary Tables 16 and 17). The colocalizations reinforced evidence supporting several genes previously implicated in T2D through detailed experimental studies, including *ADCY5*, *STARD10*, *IRS1*, *KLF14*, *SIX3*, and *TCF7L2*²⁵⁻²⁹. A single candidate effector gene was implicated at 49 T2D association signals, of which 10 colocalized with eQTLs across multiple tissues: *CEP68*, *ITGB6*, *RBM6*, *PCGF3*, *JAZF1*, *ANK1*, *ABO*, *ARHGAP19*, *PLEKHA1* and *AP3S2*. In contrast, we observed that *cis*-eQTLs at 44 signals were specific to one tissue (24 to pancreatic islets, 11 to subcutaneous adipose, five to skeletal muscle, two to visceral adipose, and one each to liver and hypothalamus), emphasizing the importance of conducting colocalization analyses across multiple tissues. Genome-wide promoter-focused chromatin confirmation capture data (pHi-C) from pancreatic islets, subcutaneous adipose, and liver (equivalent data are not available in hypothalamus and visceral adipose)³⁰⁻³² provided complementary support for several candidate effector genes (Supplementary Table 18 and Supplementary Note). These results demonstrate how the increased fine-mapping resolution afforded by our multi-ancestry meta-analysis can be integrated with diverse molecular data resources to reveal putative mechanisms underlying T2D susceptibility.

At the *BCAR1* locus, multi-ancestry fine-mapping resolved the T2D association signal to a 99% credible set of nine variants. These variants overlap a chromatin accessible snATAC-seq peak in human pancreatic acinar cells³³ and an enhancer element in human pancreatic islets that interacts with an active promoter upstream of the pancreatic exocrine enzyme chymotrypsin B2 gene *CTRB2*³¹. The observations in bulk pancreatic islets are likely to have arisen due to exocrine (acinar cell) contamination since single-cell data do not support the expression of *CTRB2* in endocrine cells (Fig. 2). The T2D association signal also colocalized with a *cis*-pQTL for circulating plasma levels of chymotrypsin B1 (*CTRB1*, $\pi_{\text{COLOC}} = 98.6\%$). Interestingly, by extending our colocalization analyses at this locus to *trans*-pQTLs, we found that variants driving the T2D association signal also regulate levels of three other pancreatic secretory enzymes produced by the acinar cells and involved in the digestion of ingested fats and proteins: carboxypeptidase B1 (*CPB1*, $\pi_{\text{COLOC}} = 98.8\%$), pancreatic lipase related protein 1 (*PLRP1*, $\pi_{\text{COLOC}} = 97.6\%$), and serine protease 2 (*PRSS2*, $\pi_{\text{COLOC}} = 98.3\%$). These observations are consistent with an effect of T2D-associated variants at this locus on gene and protein expression in the exocrine

pancreas, with consequences for pancreatic endocrine function. This is in line with a recent study³⁴ reporting rare mutations in another protein produced by the exocrine pancreas, chymotrypsin-like elastase family member 2A, which were found to influence levels of digestive enzymes and glucagon (secreted from alpha cells in pancreatic islets). Taken together, these complementary findings add to a growing body of evidence linking defects in the exocrine pancreas and T2D pathogenesis^{35,36}.

At the *PROX1* locus, multi-ancestry fine-mapping localized the two distinct association signals to just three variants (Fig. 3 and Extended Data Fig. 8). The index SNV at the first signal (rs340874, $P = 1.1 \times 10^{-18}$, $\pi > 99.9\%$) overlaps the *PROX1* promoter in both human liver and pancreatic islets^{18,29}. At the second signal, the two credible set variants map to the same enhancer active in islets and liver (rs79687284, $P = 6.9 \times 10^{-19}$, $\pi = 66.7\%$; rs17712208, $P = 1.4 \times 10^{-18}$, $\pi = 33.3\%$). Recent studies have demonstrated that the T2D-risk allele at rs17712208 (but not rs79687284) results in significant repression of enhancer activity in mouse MIN6³³ and human EndoC- β H1 beta cell models³⁷. Furthermore, this enhancer interacts with the *PROX1* promoter in islets³¹, but not in liver³². Motivated by these observations, we sought to determine whether these distinct signals impact T2D risk (via *PROX1*) in a tissue-specific manner by assessing transcriptional activity of the credible set variants (rs340874, rs79687284, and rs17712208) in human HepG2 hepatocytes and EndoC- β H1 beta cell models using *in vitro* reporter assays (Methods and Fig. 3). At the first signal, we demonstrated significant differences in luciferase activity between alleles at rs340874 in both hepatocytes (33% increase for risk allele, $P = 0.0018$) and beta cells (24% increase for risk allele, $P = 0.027$). However, at the second signal, a significant difference in luciferase activity between alleles was observed only for rs17712208 in islets (68% decrease for risk allele, $P = 0.00014$). Interestingly, there was evidence that the risk allele at rs79687284 could attenuate the effect as the combined effect of both risk alleles in the credible set was less severe. In HepG2 cells, both risk alleles increased transcription relative to wild type, although the difference for each variant alone or combined was not statistically significant. Taken together, these results suggest that likely causal variants at these distinct association signals exert their impact on T2D through the same effector gene, *PROX1*, but act in different tissue-specific manners.

Transferability of T2D GRS across diverse populations.

GRS derived from European ancestry GWAS have limited transferability into other population groups in part because of ancestry-correlated differences in the frequency and effect of risk alleles³⁸. We took advantage of the population diversity in DIAMANTE to compare the prediction performance of multi-ancestry and ancestry-specific T2D GRS constructed using lead SNVs at loci attaining genome-wide significance. We selected two studies per ancestry group as test GWAS into which the prediction performance of the GRS was assessed using trait variance explained (pseudo R^2) and odds-ratio (OR) per risk score unit. We repeated the multi-ancestry meta-regression and ancestry-specific meta-analyses, after excluding the test GWAS, and defined lead SNVs at loci attaining genome-wide significance ($P < 5 \times 10^{-9}$ for multi-ancestry GRS and $P < 5 \times 10^{-8}$ for ancestry-specific GRS). For each ancestry-specific GRS, we used allelic effect estimates for each lead SNV as weights, irrespective of the population in which the test GWAS was undertaken. However,

for the multi-ancestry GRS, we derived weights for each lead SNV that were specific to each test GWAS population by allowing for ancestry-correlated heterogeneity in allelic effects (Methods).

As expected, ancestry-specific GRS performed best in test GWAS from their respective ancestry group (Fig. 4 and Supplementary Table 19). However, for the ancestry groups with the smallest effective sample size (African, Hispanic, and South Asian), the predictive power of the ancestry-specific GRS was weak (pseudo $R^2 < 1\%$) because the number of lead SNVs attaining genome-wide significance was small. For test GWAS from these under-represented ancestry groups, the European ancestry-specific GRS outperformed the ancestry-matched GRS because: (i) more lead SNVs attained genome-wide significance in the European ancestry meta-analysis; and (ii) the T2D association signals represented by these lead SNVs are mostly shared across ancestry groups despite differing allele frequencies and LD patterns. Notwithstanding these observations, the greatest predictive power for test GWAS from all ancestry groups was achieved by the multi-ancestry GRS weighted with population-specific allelic effect estimates.

We then tested the power of the multi-ancestry GRS to predict T2D status in 129,230 individuals of Finnish ancestry from FinnGen, a population-based biobank from Finland (Methods). Because FinnGen was not part of DIAMANTE, we used association summary statistics from the complete meta-regression to derive Finnish-specific allelic effect estimates to use as weights in the multi-ancestry GRS (Extended Data Fig. 9 and Supplementary Table 20). Individuals in the top decile of the GRS were at 5.3-fold increased risk of T2D compared to those in the bottom decile. Inclusion of the multi-ancestry GRS with Finnish-specific weights to a predictive model including age, sex, and body mass index (BMI) increased the area under the receiver operating characteristic curve (AUROC) from 81.8% to 83.5%. We note that modest increases in AUROC attributable to the GRS over lifestyle/clinical factors in cross-sectional studies can mask impactful improvements in clinical performance, particularly amongst those individuals at the extremes of the GRS distribution who may have especially high lifetime disease risk and/or be prone to earlier disease onset³⁹. In FinnGen, age impacted the power of a predictive model including the T2D GRS, sex and BMI: the AUROC decreased from 86.9% in individuals under 50 years old to 73.1% in those over 80 years old (Supplementary Table 21). Each unit of the weighted GRS was associated with 1.24 years earlier age of T2D diagnosis ($P = 7.1 \times 10^{-57}$), indicating that those with a higher genetic burden are more likely to be affected earlier in life.

Positive selection of T2D risk alleles.

Previous investigations⁴⁰ have concluded that historical positive selection has not had the major impact on T2D envisaged by the thrifty genotype hypothesis⁴¹. We sought to re-evaluate the evidence for positive selection of T2D risk alleles across our expanded collection of distinct multi-ancestry association signals. We fitted demographic histories to haplotypes for each population in the 1000 Genomes Project reference panel¹³ using Relate⁴². We quantified the evidence for selection for each T2D index SNV by assessing the extent to which the mutation has more descendants than other lineages that were present

when it arose (Methods). This approach is well powered to detect positive selection acting on polygenic traits over a period of a few thousand to a few tens of thousands of years. We detected evidence of selection ($P < 0.05$) in four of the five African ancestry populations in the 1000 Genomes Project reference panel (but not other ancestry groups) towards increased T2D risk (Fig. 5). Given that T2D, itself, is likely to have been an advantageous phenotype only via pleiotropic variants acting through beneficial traits, we tested for association of index SNVs at distinct T2D signals with phenotypes available in the UK Biobank⁴³ (Methods and Extended Data Fig. 10). We found that T2D risk alleles that were also associated with increased weight (and other obesity-related traits) generally displayed more recent origin when compared to the genome-wide mutation age distribution at the same derived allele frequency ($P < 0.05$ in all African ancestry populations), consistent with positive selection (Extended Data Fig. 10). Excluding these weight-related SNVs removed the selection signature observed in African ancestry populations. These observations are consistent with positive selection of T2D risk alleles that has been driven by the promotion of energy storage and usage appropriate to the local environment⁴⁴. Outside Africa, our analysis yields no evidence for selection of T2D risk alleles. This suggests the absence of a selective advantage outside Africa, or alternatively, that the selective advantage is old and now masked in the relatively more strongly bottlenecked groups outside Africa. Further work is needed to characterize the specific pathways responsible for this adaptation and its finer-scale geographic impact.

DISCUSSION

In consideration of the global burden of T2D, the DIAMANTE Consortium assembled the most ancestrally diverse collection of GWAS of the disease to date. We implemented a powerful meta-regression approach¹⁵ to enable aggregation of GWAS summary statistics across diverse populations that allows for heterogeneity in allelic effects on disease risk that is correlated with ancestry. By representing the ancestry of each study as multidimensional and continuous axes of genetic variation, the meta-regression model is not restricted to broad continental ancestry categories and can allow for finer-scale differences between GWAS within ancestry groups⁴⁵. Our study demonstrated the advantages of applying this approach to ancestrally diverse GWAS in DIAMANTE with regard to: (i) discovery of association signals that are shared across populations, through increased sample size and by reducing the genomic control inflation due to residual stratification; (ii) defining the extent of heterogeneity in allelic effects at distinct association signals; (iii) allowing for LD-driven heterogeneity to enable fine-mapping of causal variants; and (iv) deriving population-specific weights that substantially improve the transferability of multi-ancestry GRS over ancestry-specific GRS. Our analyses considered SNVs present in the 1000 Genomes Project¹³ and Haplotype Reference Consortium¹⁴ reference panels used for imputation, which potentially excludes low-frequency population-specific variants, but which provides a uniform “backbone” of variants for fine-mapping association signals that are shared across multiple population groups. The contribution of population-specific variants that do not overlap reference panels are more fully assessed in complementary ancestry-specific meta-analyses, such as those in European and East Asian components of DIAMANTE^{6,10}. Further

development of fine-mapping methods is required to localize such population-specific causal variants in multi-ancestry meta-analysis⁴⁶.

Our study has extended knowledge of T2D genetics over previous efforts that include GWAS that have contributed to our multi-ancestry meta-analysis^{6,10,11}, demonstrating the opportunities to deliver new biological insights and identify novel target genes and mechanisms through which genetic variation impacts on disease risk. Annotation-informed multi-ancestry fine-mapping resolved 54.4% of distinct T2D association signals to a single variant with >50% posterior probability. Through integration of these fine-mapping data with molecular QTL resources, we identified a total of 117 candidate causal genes at T2D loci, of which 40 were not reported in complementary analyses undertaken in previous efforts (Supplementary Note). Formal Bayesian colocalization analyses across diverse tissues highlighted complex cell-type specific mechanisms through which regulatory variants at non-coding T2D association signals impact disease risk, exemplified by the *BCAR1* and *PROX1* loci, and lay the foundations for future functional investigations. Our study is the first to demonstrate the advantages of a GRS derived from multi-ancestry meta-regression for T2D prediction across five major ancestry groups. Finally, we built on our expanded collection of distinct multi-ancestry association signals to demonstrate evidence of positive selection of T2D risk alleles in African populations that may have been driven by the promotion of energy storage and usage through adaptation to the local environment.

Multi-ancestry meta-analysis maximizes power to detect association signals that are shared across ancestry groups. However, by modelling heterogeneity in allelic effects across ancestries, our meta-regression approach can also allow for association signals that are driven by ancestry-specific causal variants, although power will be limited by the sample size available in that ancestry group. Ancestry-specific variants tend to have lower frequency, with the result that discovery of T2D associations that are unique to African, Hispanic, or South Asian ancestry groups in our study will have been limited to those with relatively large effects. To address this limitation, it remains essential that the human genetics research community continues to bolster GWAS collections in underrepresented populations that often suffer the greatest burden of disease and to further expand diversity in imputation reference panels, as exemplified by the Trans-Omics for Precision Medicine (TOPMed) Program⁴⁷. Increasing diversity in genetic research will ultimately provide a more comprehensive and refined view of the genetic contribution to complex human traits, powering understanding of the molecular and biological processes underlying common diseases, and offering the most promising opportunities for clinical translation of GWAS findings to improve global public health.

METHODS

Ethics statement.

All human research was approved by the relevant Institutional Review Boards and conducted according to the Declaration of Helsinki. All participants provided written informed consent. Study-level ethics statements are provided in the Supplementary Note.

Study-level analyses.

Individuals were assayed with a range of GWAS genotyping arrays, with sample and SNV quality control (QC) undertaken within each study (Supplementary Tables 2 and 4). Most GWAS were undertaken with individuals from one ancestry group (Supplementary Table 1), where population outliers were excluded using self-reported and genetic ancestry. For the remaining multi-ancestry GWAS (Supplementary Table 1), individuals were first assigned to an ancestry group using both self-reported and genetic ancestry, and analyses were then undertaken separately within each ancestry group. For each ancestry-specific GWAS, samples were pre-phased and imputed up to reference panels from the 1000 Genomes Project (phase 1, March 2012 release; phase 3, October 2014 release)^{12,13}, Haplotype Reference Consortium¹⁴, or population-specific whole-genome sequencing⁴⁸⁻⁵⁰ (Supplementary Table 4). SNVs with poor imputation quality and/or minor allele count <5 were excluded from downstream association analyses (Supplementary Table 4). Association with T2D was evaluated in a regression framework, under an additive model in the dosage of the minor allele, with adjustment for age and sex (where appropriate), and additional study-specific covariates (Supplementary Table 4). Analyses accounted for structure (population stratification and/or familial relationships) by: (i) excluding related samples and adjusting for principal components derived from a genetic relatedness matrix (GRM) as additional covariates in the regression model; or (ii) incorporating a random effect for the GRM in a mixed model (Supplementary Table 4). Allelic effects and corresponding standard errors that were estimated from a linear (mixed) model were converted to the log-odds scale⁵¹. Study-level association summary statistics (*P*-values and standard error of allelic log-ORs) were corrected for residual structure, not accounted for in the regression analysis, by means of genomic control⁵² if the inflation factor was >1 (Supplementary Table 4).

Multi-ancestry meta-analyses.

To account for the different reference panels used for imputation, we considered autosomal bi-allelic SNVs that overlap the 1000 Genomes Project reference panel (phase 3, October 2014 release)¹³ and the Haplotype Reference Consortium reference panel¹⁴. We considered only those SNVs with MAF > 0.5% in haplotypes in at least one of the five ancestry groups (Supplementary Table 22) in the 1000 Genomes Project (phase 3, October 2014 release)¹³. We excluded SNVs that differed in allele frequency by >20% when comparing reference panels in the same subsets of samples.

The most powerful methods for discovery of novel loci through multi-ancestry meta-analysis allow for potential allelic effect heterogeneity between ancestry groups that cannot be accommodated in a fixed-effects model⁵³. Random-effects meta-analysis allows for “unstructured” heterogeneity, but cannot allow for the expectation that GWAS from the same ancestry group are likely to have more similar allelic effects than those from different ancestry groups. Some of these limitations could be addressed with a two-stage hierarchical model (within and then between ancestry). However, we preferred a meta-regression approach, implemented in MR-MEGA¹⁵, which models allelic effect heterogeneity that is correlated with genetic ancestry by including axes of genetic variation as covariates to capture ancestral diversity between GWAS. We constructed a distance matrix of mean effect allele frequency differences between each pair of GWAS across a subset of 386,563 SNVs

reported in all studies. We implemented multi-dimensional scaling of the distance matrix to obtain three principal components that defined axes of genetic variation to separate GWAS from the five ancestry groups (Extended Data Fig. 2).

For each SNV, we modelled allelic log-ORs across GWAS in a linear regression framework, weighted by the inverse of the variance of the effect estimates, incorporating the three axes of genetic variation as covariates. We tested for: (i) association with T2D allowing for allelic effect heterogeneity between GWAS that is correlated with ancestry; (ii) heterogeneity in allelic effects on T2D between GWAS that is correlated with ancestry; and (iii) residual allelic effect heterogeneity between GWAS due to unmeasured confounders. We corrected the meta-regression association P -values for inflation due to residual structure between GWAS using genomic control adjustment (allowing for four degrees of freedom): $\lambda_{TA} = 1.052$. We included SNVs reported in 50% of the total effective sample size ($N_{TA} = 246,095$) in downstream analyses.

We also aggregated association summary statistics across GWAS via fixed-effects meta-analysis using METAL⁵⁴ and random-effects (RE2 model) meta-analysis using METASOFT⁵⁵. Both meta-analyses were based on inverse-variance weighting of allelic log-ORs to obtain effect size estimates. We corrected standard errors for inflation due to residual structure between GWAS by genomic control adjustment: $\lambda_{TA}^{FE} = 1.253$ and $\lambda_{TA}^{RE} = 1.253$.

We assessed evidence for heterogeneity in allelic effects between GWAS by Cochran's Q statistic.

Defining T2D loci.

We initially selected lead SNVs attaining genome-wide significant evidence of association ($P < 5 \times 10^{-8}$) in the multi-ancestry meta-regression that were separated by at least 500 kb. Loci were first defined by the flanking genomic interval mapping 500 kb up- and downstream of lead SNVs. Then, where lead SNVs were separated by less than 1 Mb, the corresponding loci were aggregated as a single locus. The lead SNV for each locus was then selected as the SNV with minimum association P -value.

Genome-wide significance threshold.

We considered haplotypes from the 1000 Genomes Project reference panel (phase 3, October 2014 release)¹³. We extracted autosomal bi-allelic SNVs that overlapped between reference panels used in study-level analyses. We estimated the effective number of independent SNVs across ancestry groups using LD-pruning in PLINK⁵⁶ to be 9,966,662 at $r^2 > 0.5$ ⁵⁷. We therefore chose a multi-ancestry genome-wide significance threshold by Bonferroni correction for the effective number of SNVs as $P < 5 \times 10^{-9}$. Exemplar power calculations are provided in the Supplementary Note.

Dissection of distinct multi-ancestry association signals.

We used iterative approximate conditioning, implemented in GCTA⁵⁸, making use of forward selection and backward elimination, to identify index SNVs at multi-ancestry genome-wide significance ($P < 5 \times 10^{-9}$). We used haplotypes from the 1000 Genomes Project reference panel (phase 3, October 2014 release)¹³ that were specific to each ancestry

group (Supplementary Table 22) as a reference for LD between SNVs across loci in the approximate conditional analysis. Details of the iterative approximate conditioning are provided in the Supplementary Note.

Ancestry-specific meta-analyses.

We aggregated association summary statistics across GWAS via fixed-effects meta-analysis using METAL⁵⁴ based on inverse-variance weighting of allelic log-OR to obtain effect size estimates. Details are provided in the Supplementary Note.

Fine-mapping resolution.

Within each locus, we approximated the Bayes' factor⁵⁹, Λ_{jj} , in favor of T2D association of the j th SNV at the i th distinct association signal using summary statistics from: (i) the multi-ancestry meta-regression; (ii) the European ancestry-specific meta-analysis; and (iii) the combined East Asian and European ancestry meta-analysis. For loci with a single association signal, association summary statistics were obtained from unconditional analysis. For loci with multiple distinct association signals, association summary statistics were obtained from approximate conditional analyses. Details of the derivation of approximate Bayes' factors are provided in the Supplementary Note. The posterior probability for the j th SNV at the i th distinct signal was then given by $\pi_{ij} \propto \Lambda_{ij}$. We derived a 99% credible set⁶⁰ for the i th distinct association signal by: (i) ranking all SNVs according to their posterior probability π_{ij} ; and (ii) including ranked SNVs until their cumulative posterior probability attains or exceeds 0.99.

Down-sampled multi-ancestry meta-regression.

We selected GWAS contributing to the multi-ancestry meta-regression to approximate the effective sample size of the European ancestry-specific meta-analysis and maintain the distribution of effective sample size across ancestry groups (Supplementary Table 10). The selected GWAS are summarized in the Supplementary Note. We conducted a “down-sampled” multi-ancestry meta-regression, implemented in MR-MEGA¹⁵, for the selected studies. For each SNV, we modelled allelic log-ORs across GWAS in a linear regression framework, weighted by the inverse of the variance of the effect estimates, incorporating the same three axes of genetic variation as covariates (Extended Data Fig. 2). We corrected the meta-regression association P -values for inflation due to residual structure between the selected GWAS using genomic control adjustment (allowing for four degrees of freedom): $\lambda_{TA^*} = 1.012$. For each distinct association signal identified in the complete multi-ancestry meta-regression, we derived a 99% credible set⁶⁰ using association summary statistics from the down-sampled multi-ancestry meta-regression. Details of the fine-mapping procedure are provided in the Supplementary Note.

Enrichment of T2D association signals in genomic annotations.

We mapped each SNV across T2D loci to three categories of functional and regulatory annotations: (i) genic regions, as defined by the GENCODE Project⁶¹, including protein-coding exons, and 3' and 5' UTRs as different annotations; (ii) chromatin immunoprecipitation sequence (ChIP-seq) binding sites for 165 transcription factors (161 proteins

from the ENCODE Project⁶² and four additional factors assayed in primary pancreatic islets⁶³); and (iii) 13 unique and recurrent chromatin states, including promoter, enhancer, transcribed, and repressed regions, in four T2D-relevant tissues¹⁸ (pancreatic islets, liver, adipose, and skeletal muscle). This resulted in a total of 220 genomic annotations for downstream enrichment analyses. We used fGWAS⁶⁴ to identify a joint model of enriched annotations across distinct T2D association signals from the multi-ancestry meta-regression. Details are provided in the Supplementary Note.

Annotation informed fine-mapping.

Within each locus, for each distinct signal, we recalibrated the posterior probability of driving the T2D association for each SNV under an annotation-informed prior derived from the joint model of enriched annotations identified by fGWAS. Specifically, for the j th SNV at the i th distinct signal, the posterior probability $\pi_{ij} \propto \gamma_j \Lambda_{ij}$, where Λ_{ij} is the Bayes' factor in favor of T2D association. In this expression, the relative annotation-informed prior for the SNV is given by

$$\gamma_j = \exp\left[\sum_k \hat{\beta}_k z_{jk}\right],$$

where the summation is over the enriched annotations, $\hat{\beta}_k$ is the estimated log-fold enrichment of the k th annotation from the final joint model, and z_{jk} is an indicator variable taking the value 1 if the j th SNV maps to the k th annotation, and 0 otherwise. We derived a 99% credible set⁶⁰ for the i th distinct association signal by: (i) ranking all SNVs according to their posterior probability π_{ij} ; and (ii) including ranked SNVs until their cumulative posterior probability attains or exceeds 0.99.

Dissection of molecular QTLs in diverse tissues.

We accessed association summary statistics for molecular QTLs in diverse tissues from three published resources: (i) 3,622 circulating plasma proteins in 3,301 healthy blood donors of European ancestry from the INTERVAL Study²¹; (ii) pancreatic islet expression in 420 individuals of European ancestry from the InsPIRE Consortium²³; and (iii) multi-tissue expression in 620 donors from the GTEx Project (release v7)²², including subcutaneous adipose (328 samples), visceral adipose (273 samples), brain hypothalamus (108 samples), liver (134 samples), and skeletal muscle (421 samples). We defined *cis*-molecular QTL as mapping within 1 Mb of the transcription start site of the gene. Recognising that molecular QTLs may also be driven by multiple causal variants, we dissected signals for each significant *cis*- and *trans*-pQTL ($P < 1.5 \times 10^{-11}$) and for each significant *cis*-eQTL (FDR q -value $< 5\%$) via approximate conditional analyses implemented in GCTA⁵⁸. We used a genotype reference panel of 6,000 unrelated individuals of white British origin, randomly selected from the UK Biobank⁴³, to model LD between SNVs. We excluded SNVs from the reference panel with poor imputation quality (info < 0.4) and/or significant deviation from Hardy-Weinberg equilibrium ($P < 10^{-6}$). We first identified index SNVs for each distinct molecular QTL signal using the "--cojo-slc" option: $P < 1.5 \times 10^{-11}$ for *cis*- and *trans*-pQTLs; and $P < 5 \times 10^{-8}$ for *cis*-eQTLs. For each molecular QTL with multiple

index SNVs, we dissected each distinct signal using GCTA, removing each index SNV, and adjusting for the remainder, using the “--cojo-cond” option.

Colocalization of T2D associations and molecular QTLs.

For each distinct T2D association signal, we used COLOCv3.1²⁴ to assess the evidence for colocalization with: (i) each distinct *cis*- and *trans*-pQTL signal; and (ii) each distinct *cis*-eQTL signal across tissues. COLOC assumes that at most one variant is causal for each distinct T2D association and each distinct molecular QTL, which is reasonable after deconvolution of signals via approximate conditional analyses. Under this assumption, there are five hypotheses: association with neither T2D nor the molecular QTL (H_0); association only with T2D (H_1) or the molecular QTL (H_2); or association with both T2D and the molecular QTL, driven either by two different causal variants (H_3) or by the same causal variant (H_4). We assumed the default prior probabilities of: (i) 10^{-4} that a variant is causal only for T2D or only for the molecular QTL; and (ii) 10^{-6} that a variant is causal for both T2D and the molecular QTL. To take account of our annotation-informed prior model of causality, we then replaced the Bayes' factor in favor of T2D association, A_{ij} , for the j th SNV at the i th distinct signal by $\pi_{ij} \Psi_j$, where $\Psi_j = \prod_i A_{ij}$ is the total Bayes' factor for the signal. For the molecular QTLs, approximate Bayes' factors in favor of association for each variant were derived using Wakefield's method⁶⁵. Under this model, COLOC then estimates the posterior probability of colocalization of the T2D association and molecular QTL (i.e. hypothesis H_4 , denoted π_{COLOC}).

Plasmid transfection and luciferase reporter assay.

We experimentally validated 99% credible set variants for distinct T2D association signals at the *PROX1* locus using a luciferase reporter assay. Briefly, human EndoC- β H1 cells⁶⁶ and human liver cells were grown at 50-60% confluence in 24-well plates and were transfected (2×10^5 EndoC- β H1 cells/well and 5×10^4 HepG2 cells/well) with 500 ng of empty pGL3-Promoter vector (Promega, Charbonnières, France) or pGL3-Promoter-PROX_insert with FuGENE HD (Roche Applied Science, Meylan, France) using a FuGENE:DNA ratio of 6:1 according to the manufacturer's instructions. Details are provided in the Supplementary Note and at <https://www.promega.co.uk/products/luciferase-assays/genetic-reporter-vectors-and-cell-lines/pgl3-luciferase-reporter-vectors/?catNum=E1751>. Luciferase activities were measured 48 hours after transfection using the Dual-Luciferase Reporter Assay kit (Promega) according to the manufacturer's instructions, in half-volume 96-well tray format on an Enspire Multimode Plate Reader (PerkinElmer). The Firefly luciferase activity was normalized to the Renilla luciferase activity obtained by cotransfection of 10 ng of the pGL4.74[hRluc/TK] Renilla luciferase vector (Promega). All experiments were performed in triplicate in three different passages of each cell type. Differences in luciferase activity between groups were tested using two-tailed two-sample *t*-tests, where $P < 0.05$ was considered statistically significant.

Transferability of GRS across ancestry groups.

We selected two studies per ancestry group as test GWAS, prioritizing those with larger effective sample sizes and greater genetic diversity (Supplementary Note). We repeated the multi-ancestry meta-regression, after excluding the ten test GWAS, incorporating the

same three axes of genetic variation as covariates to account for ancestry. The association P -values from this “reduced” meta-regression were then corrected for inflation due to residual structure between GWAS by means of genomic control adjustment (allowing for four degrees of freedom): $\lambda_{TA} = 1.037$. SNVs reported in 50% of the total effective sample size of the “reduced” meta-regression ($N_{TE} = 179,074$) were included in downstream analyses. We identified loci attaining genome-wide significant evidence of association ($P < 5 \times 10^{-9}$) in the “reduced” meta-regression, and the lead SNV for each locus was selected as the variant with minimum association P -value. For each test GWAS, we next estimated population-specific “predicted” allelic effects for each lead SNV to be used as weights in the GRS. We also repeated each of the ancestry-specific fixed-effects meta-analyses after excluding the ten test GWAS, and identified lead SNVs attaining genome-wide significant evidence of association ($P < 5 \times 10^{-8}$). For each test GWAS, we estimated the OR per unit of the population-specific multi-ancestry GRS and each ancestry-specific weighted GRS, and the corresponding percentage of T2D variance explained (pseudo R^2). Details are provided in the Supplementary Note.

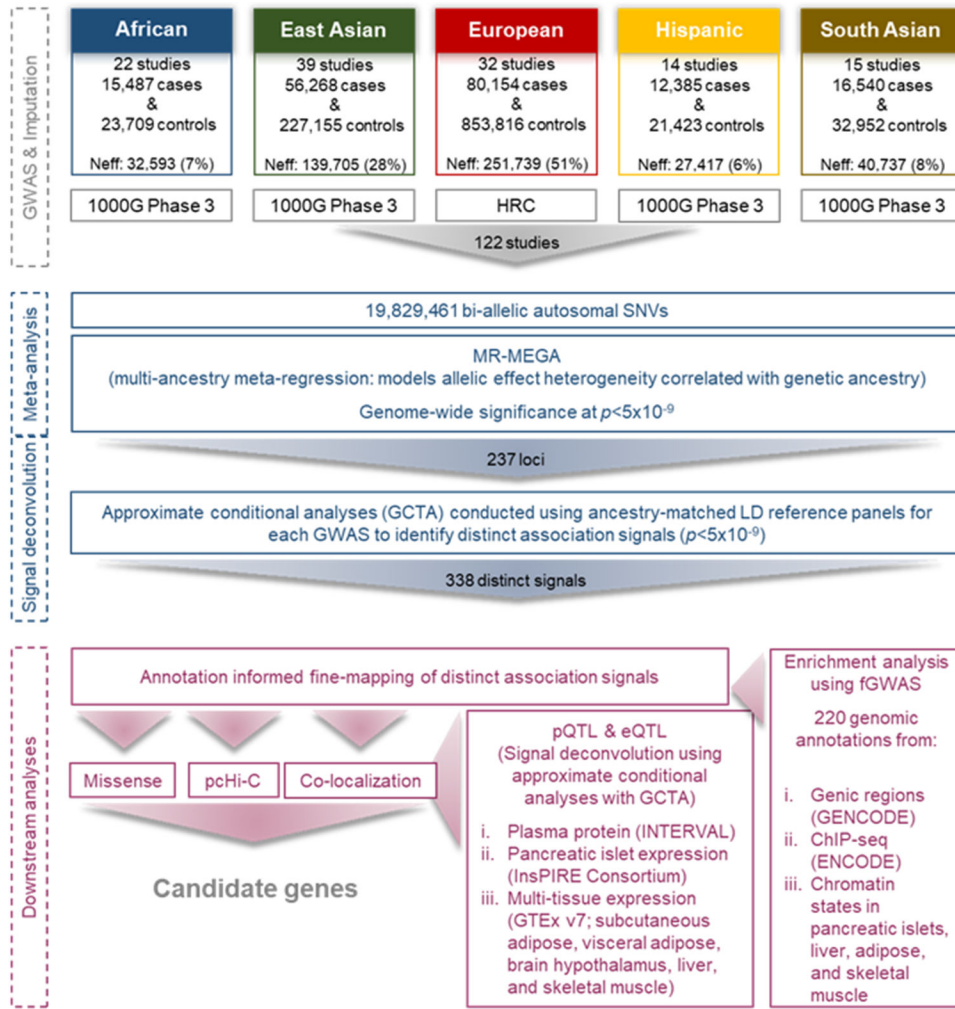
Predictive power of GRS in FinnGen.

Individuals from FinnGen were genotyped with Illumina and Affymetrix arrays, and were imputed up to the Finnish population-specific reference panel (SISu version 3). We excluded individuals due to non-Finnish ancestry, relatedness, or missing age and/or sex. We derived Finnish-specific “predicted” allelic effect estimates for each lead SNV from the multi-ancestry meta-regression to be used as weights in calculating the centred GRS for each individual. We excluded lead SNVs from the GRS that were not reported in FinnGen. We excluded individuals with missing T2D status or BMI from subsequent analyses, resulting in a total of 18,111 affected individuals and 111,119 unaffected individuals. We calculated the variance in T2D status explained (pseudo R^2) and the AUROC (calculated with a 10-fold cross-validation) for models including BMI and/or GRS. We also conducted age-stratified analyses and tested for association of the GRS with age of T2D diagnosis. Details are provided in the Supplementary Note.

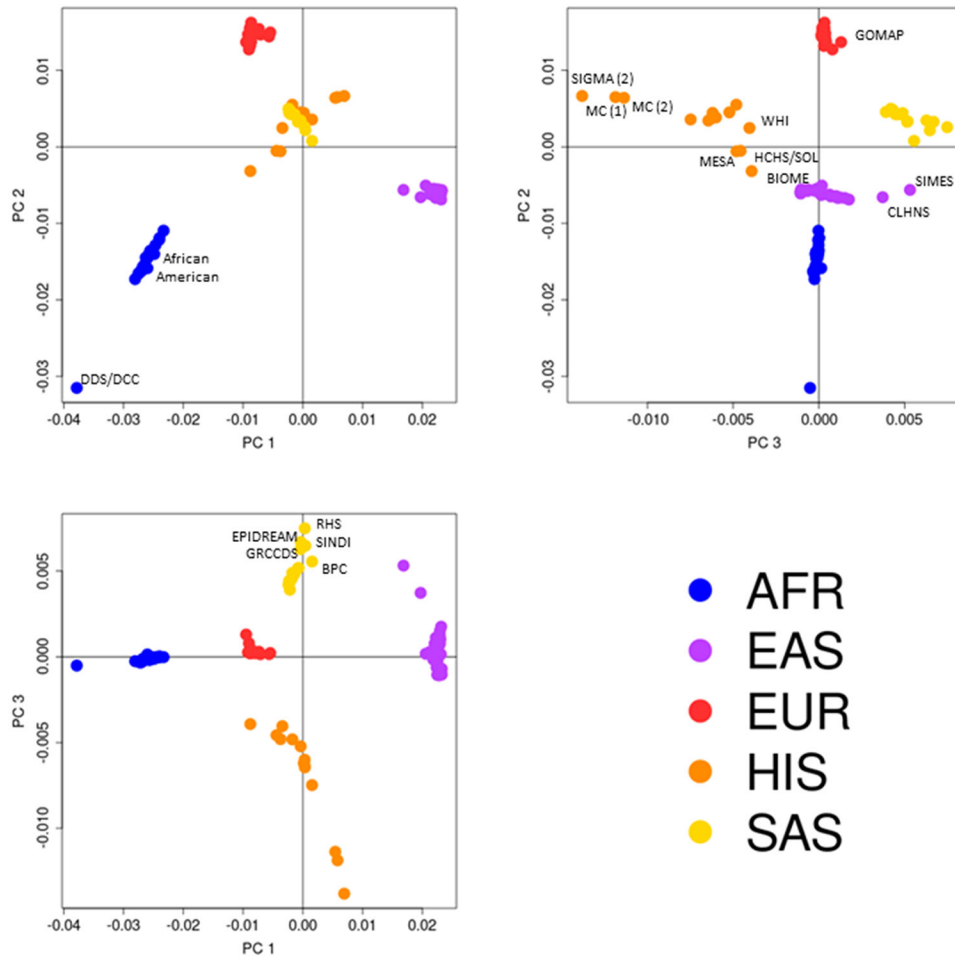
Selection analyses.

We used Relate⁴² to reconstruct genealogies for haplotypes from the 1000 Genomes Project reference panel (phase 3, October 2014 release)¹³, separately for each population, after excluding African American and admixed American populations in whom high levels of admixture are likely to confound selection evidence. We then used P -values calculated for selection evidence for any variant that segregated in the population and passed quality control filters⁴², which quantify the extent to which the mutation has more descendants than other lineages that were present when it arose. We tested for evidence of selection for index SNVs for distinct T2D association signals, which were partitioned into two groups, risk and protective, according to the direction of the allelic effect when aligned to the derived allele. We also tested for selection on a range of traits available in the UK Biobank⁴³ at the subset of index SNVs for which the derived allele increased risk of T2D. Details are provided in the Supplementary Note.

Extended Data

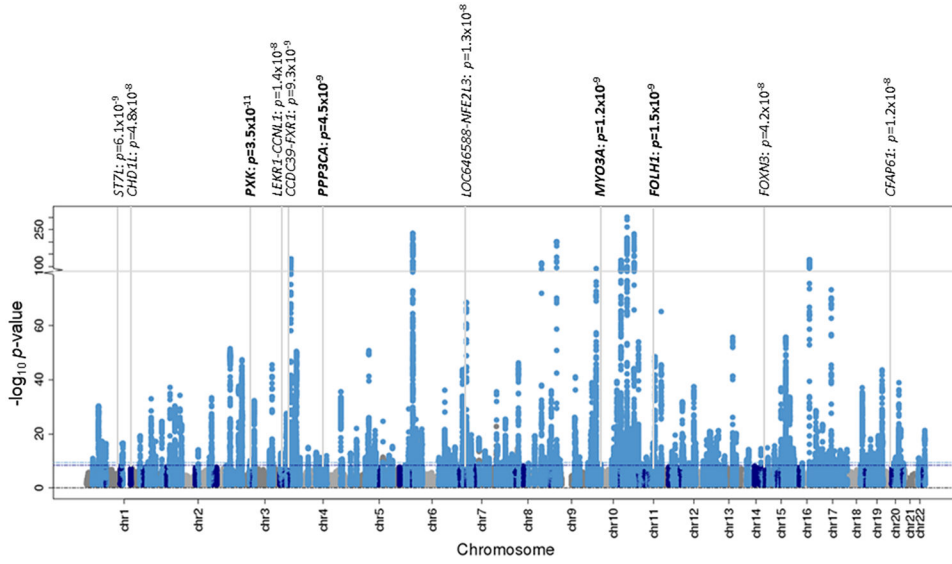


Extended Data Fig. 1. Study overview.
Summary of data resources and downstream analyses to identify candidate causal genes at T2D susceptibility loci.



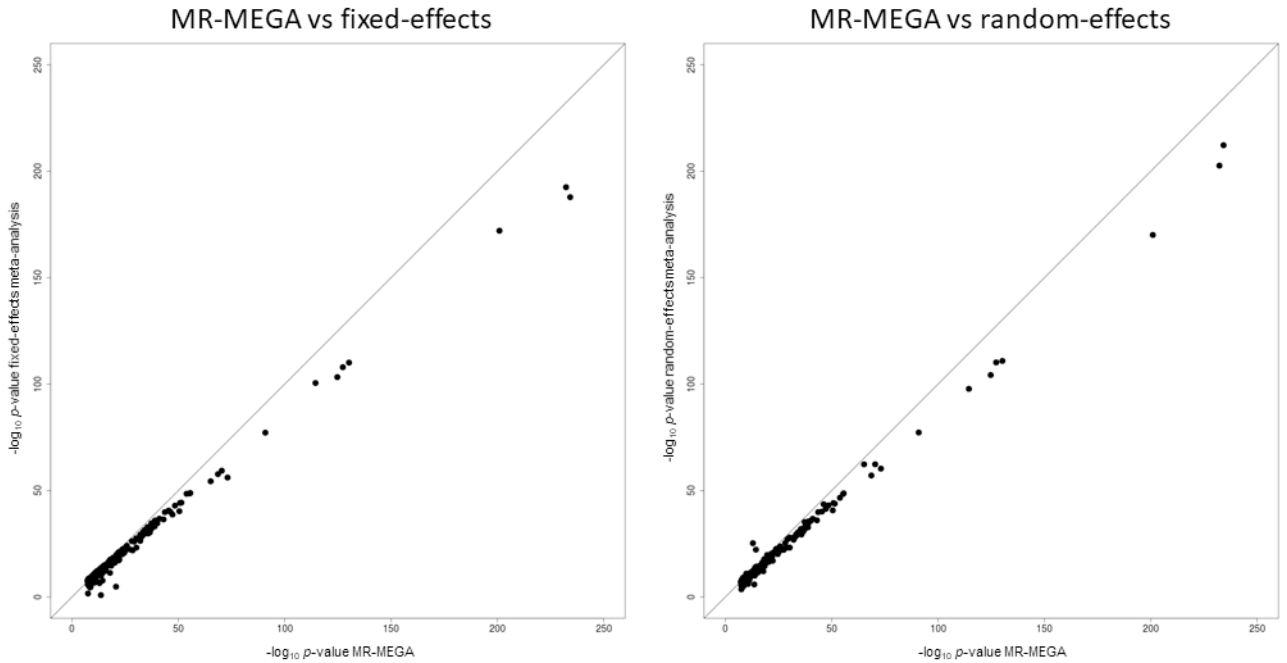
Extended Data Fig. 2. Axes of genetic variation separating GWAS of T2D across diverse populations.

The first three axes of genetic variation (PC 1, PC 2 and PC 3) from multi-dimensional scaling of the Euclidean distance matrix between populations are sufficient to separate five ancestry groups: African (AFR), East Asian (EAS), European (EUR), Hispanic (HIS) and South Asian (SAS). The second axis of genetic variation (PC 2) separates African American and continental African GWAS. The third axis of genetic variation (PC 3) reveals finer-scale differences between GWAS within ancestry groups: Hispanic studies with a greater proportion of American ancestry (SIGMA (2), MC (1) and MC (2)) or African ancestry (WHI, MESA, HCHS/SOL and BIOME); East Asian studies of Chinese, Japanese and Korean ancestry from those of Malay and Filipino ancestry (SITES and CLHNS); South Asian studies of Sri Lankan, Bangladeshi and South Indian ancestry (RHS, EPIDREAM, SINDI, GRCCDS and BPC) from those of North Indian and Pakistani ancestry; and Northern European ancestry studies from the study of Greek ancestry from Southern Europe (GOMAP). GWAS were aligned to ancestry groups based on self-report at the study level.



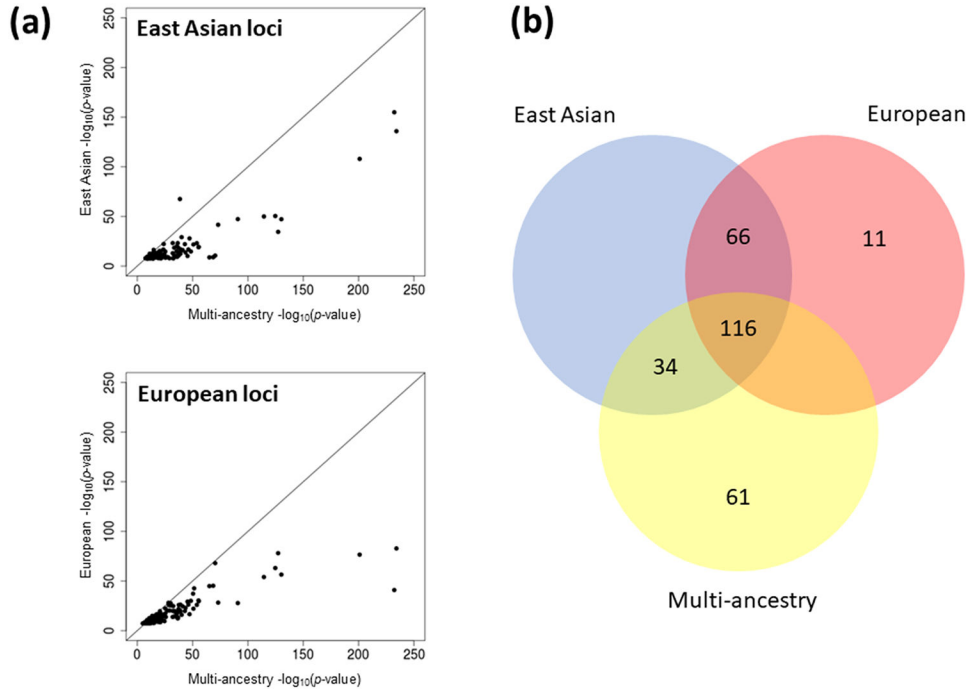
Extended Data Fig. 3. Manhattan plot of genome-wide T2D association from multi-ancestry meta-regression (MR-MEGA) of up to 180,834 cases and 1,159,055 controls.

Each point represents an SNV passing quality control in the multi-ancestry meta-regression, plotted with their association P -value (on a $-\log_{10}$ scale, truncated at 300) as a function of genomic position (NCBI build 37). Association signals attaining genome-wide significance are highlighted in pale blue ($P < 5 \times 10^{-9}$) and dark blue ($P < 5 \times 10^{-8}$). The names of novel loci names are highlighted with their association P -value from the multi-ancestry meta-regression.



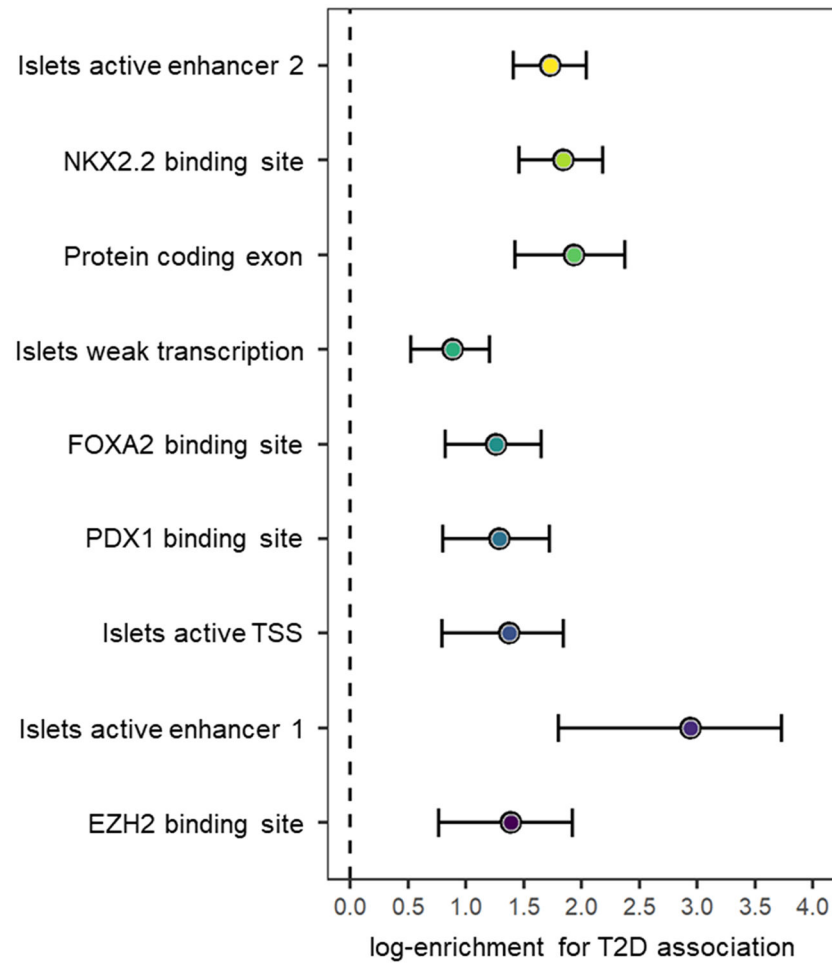
Extended Data Fig. 4. Comparison of association P -values at lead SNVs at T2D loci between multi-ancestry meta-regression (MR-MEGA), fixed-effects meta-analysis and random-effects (RE2) meta-analysis of up to 180,834 cases and 1,159,055 controls.

Each point corresponds to an SNV, plotted according to P -values (on a $-\log_{10}$ scale) from MR-MEGA on the x -axis and fixed- or random-effects meta-analysis on the y -axis. SNVs below the $y = x$ line demonstrate stronger association with MR-MEGA. The lead SNV at the *TCF7L2* locus has been removed to improve clarity of presentation.



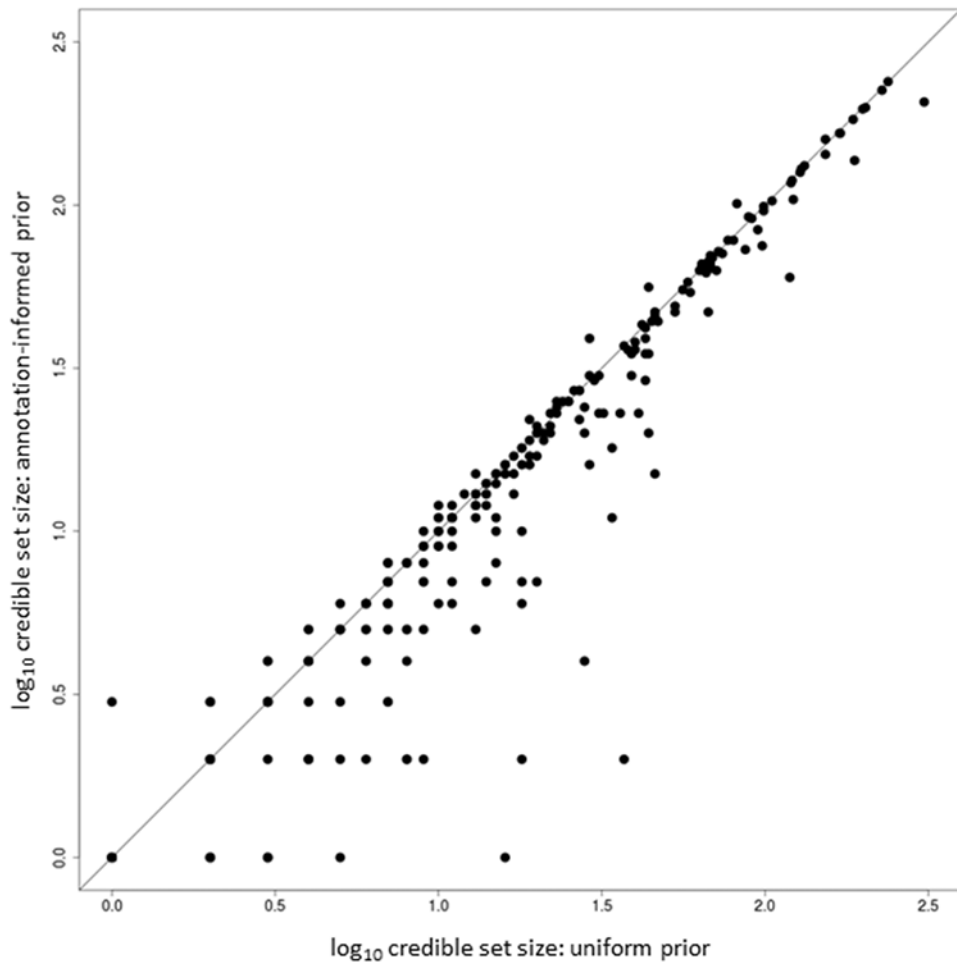
Extended Data Fig. 5. Comparison of loci identified at genome-wide significance ($P < 5 \times 10^{-8}$) in multi-ancestry meta-regression (180,834 cases and 1,159,055 controls), and East Asian and European ancestry-specific meta-analyses (56,268 cases and 227,155 controls, and 80,154 cases and 853,816 controls, respectively).

a, Association P -values at loci identified in East Asian and European ancestry-specific meta-analyses. Each point corresponds to a locus, plotted according to the P -value (on a $-\log_{10}$ scale) for the lead SNP in the multi-ancestry meta-regression on the x -axis and the lead SNP in the ancestry-specific meta-analysis on the y -axis. The *TCF7L2* locus has been removed to improve clarity of presentation. Loci plotted below the $y = x$ line show stronger evidence for association in the multi-ancestry meta-regression. **b**, Overlap of loci identified in multi-ancestry meta-regression and ancestry-specific meta-analyses.

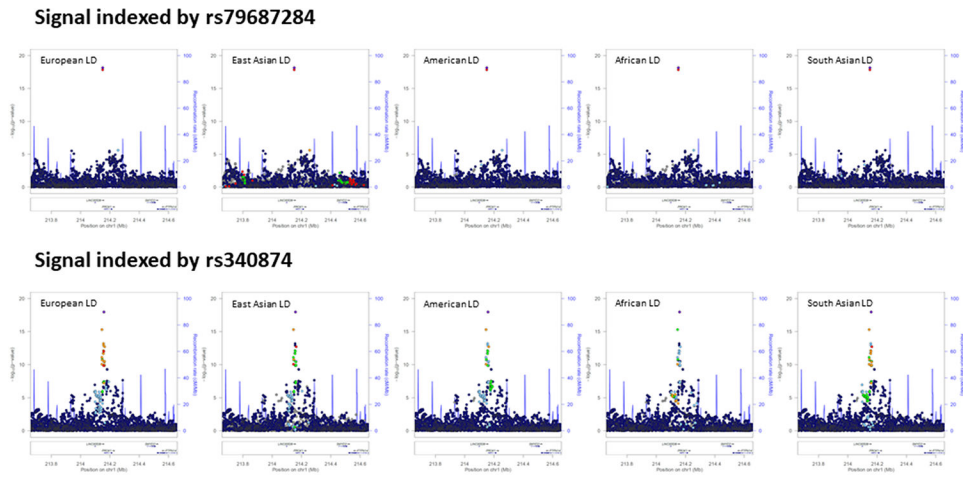


Extended Data Fig. 6. Summary statistics from joint fGWAS model of enriched functional and regulatory annotations across distinct T2D association signals from multi-ancestry meta-regression (MR-MEGA) of up to 180,834 cases and 1,159,055 controls.

Each point corresponds to an annotation, plotted for the log-enrichment for T2D association on the x -axis, with bars representing the corresponding 95% confidence interval (CI).

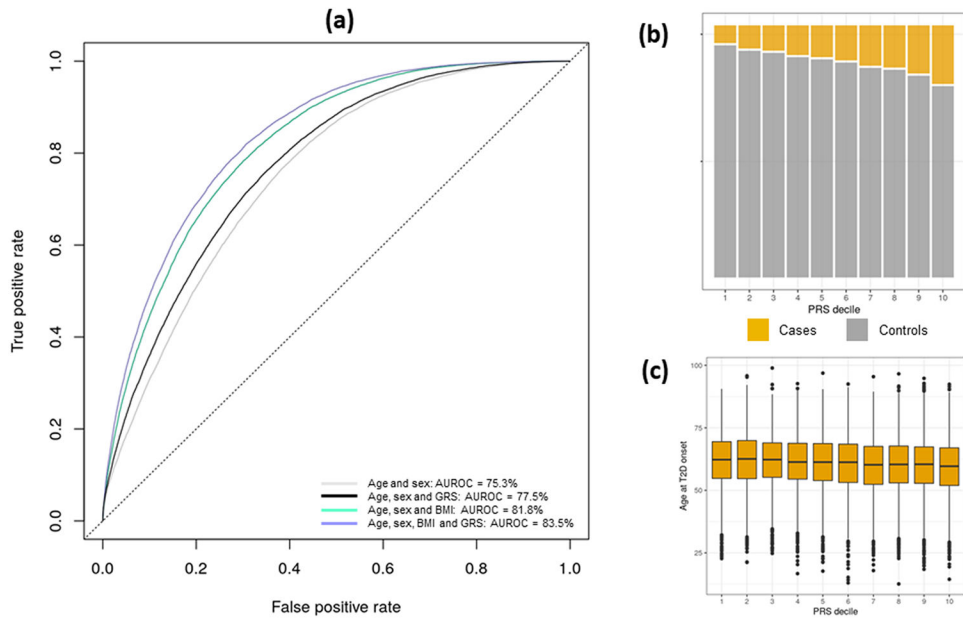


Extended Data Fig. 7. Comparison of number of SNVs in 99% credible set for distinct association signals for T2D obtained from the multi-ancestry meta-regression of 180,834 cases and 1,159,055 controls under uniform and annotation-informed prior models of causality. Each point corresponds to a distinct association signal, plotted according to the \log_{10} credible set size under the uniform prior on the x -axis and the \log_{10} credible set size under the annotation-informed prior on the y -axis. The 144 (42.6%) signals below the $y = x$ line were more precisely fine-mapped under the annotation-informed prior.



Extended Data Fig. 8. Differences in LD structure between ancestry groups at the *PROXI* locus for distinct association signals from multi-ancestry meta-regression (MR-MEGA) of up to 180,840 cases and 1,159,185 controls.

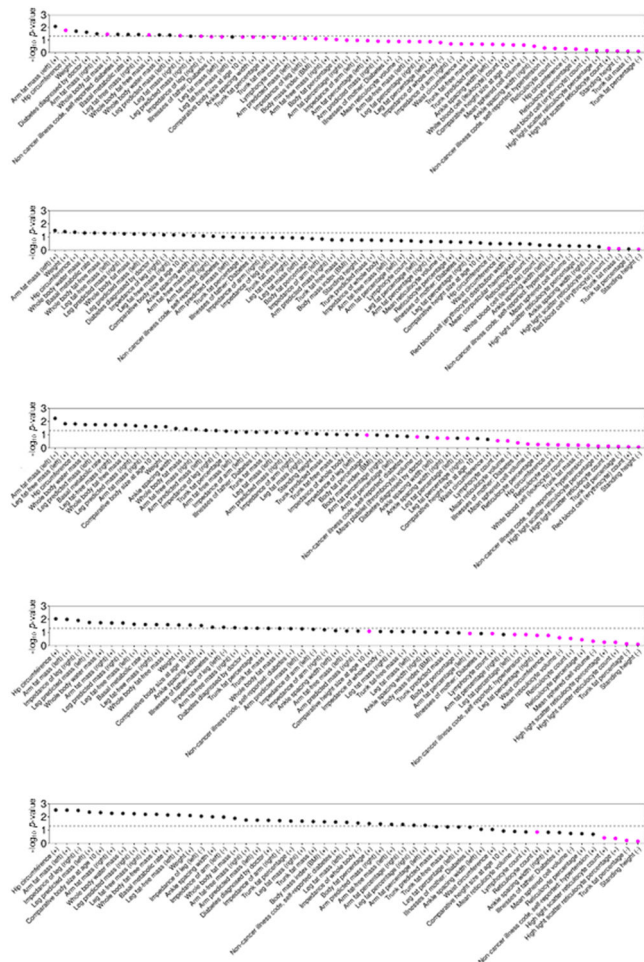
Each point represents an SNV passing quality control in the multi-ancestry meta-regression (after conditional analysis), plotted with their association P -value (on a \log_{10} scale) as a function of genomic position (NCBI build 37). The index SNV is represented by the purple symbol. The color coding of all other SNVs indicates LD with the index variant in the ancestry-matched reference haplotypes from the 1000 Genomes Project panel: red, $r^2 \geq 0.8$; gold, $0.6 \leq r^2 < 0.8$; green, $0.4 \leq r^2 < 0.6$; cyan, $0.2 \leq r^2 < 0.4$; blue, $r^2 < 0.2$; grey, r^2 unknown. Recombination rates are estimated from Phase II HapMap and gene annotations are taken from the University of California Santa Cruz genome browser.



Extended Data Fig. 9. Power of multi-ancestry GRS to predict T2D status in 129,230 individuals of Finnish ancestry from FinnGen.

a. Age under receiver operating characteristic curve (AUROC) after adding BMI and GRS to a baseline model adjusting for age and sex. **b.** Prevalence of T2D across GRS deciles. **c.**

Boxplot of the distribution of age at T2D diagnosis across GRS deciles: box defines upper quartile, median and lower quartile, bars define maximum and minimum values within 1.5 x interquartile range of the upper and lower quartiles, other points are outliers.



Extended Data Fig. 10. Evidence for selection from Relate in African ancestry populations of subsets of T2D risk variants (effect aligned to derived allele) that are associated with other traits available in the UK Biobank.

Nominal evidence for selection ($P < 0.05$) is indicated by the dashed line. The color of each point indicates the evidence for selection of subsets of T2D risk variants that are not associated with the other trait: $P < 0.05$ (pink) and $P > 0.05$ (black). Population abbreviations: ESN, Esan in Nigeria; GWD, Gambian in Western Divisions in the Gambia; LWK, Luhya in Webuye, Kenya; MSL, Mende in Sierra Leone; YRI, Yoruba in Ibadan, Nigeria.

Supplementary Material

Refer to Web version on PubMed Central for supplementary material.

Authors

Anubha Mahajan^{1,2,278,†}, Cassandra N. Spracklen^{3,4,*}, Weihua Zhang^{5,6,*}, Maggie C. Y. Ng^{7,8,9,*}, Lauren E Petty^{7,*}, Hidetoshi Kitajima^{2,10,11,12,*}, Grace Z. Yu^{1,2,*}, Sina Rüeger^{13,*}, Leo Speidel^{14,15,*}, Young Jin Kim¹⁶, Momoko Horikoshi¹⁷, Josep M. Mercader^{18,19,20}, Daniel Taliun²¹, Sanghoon Moon¹⁶, Soo-Heon Kwak²², Neil R. Robertson^{1,2}, Nigel W. Rayner^{1,2,23,24}, Marie Loh^{5,25,26}, Bong-Jo Kim¹⁶, Joshua Chiou^{27,279}, Irene Miguel-Escalada^{28,29}, Pietro della Briotta Parolo¹³, Kuang Lin³⁰, Fiona Bragg^{30,31}, Michael H. Preuss³², Fumihiko Takeuchi³³, Jana Nano³⁴, Xiuqing Guo³⁵, Amel Lamri^{36,37}, Masahiro Nakatochi³⁸, Robert A. Scott³⁹, Jung-Jin Lee⁴⁰, Alicia Huerta-Chagoya^{41,280}, Mariaelisa Graff⁴², Jin-Fang Chai⁴³, Esteban J Parra⁴⁴, Jie Yao³⁵, Lawrence F. Bielak⁴⁵, Yasuharu Tabara⁴⁶, Yang Hai³⁵, Valgerdur Steinthorsdottir⁴⁷, James P. Cook⁴⁸, Mart Kals⁴⁹, Niels Garup⁵⁰, Ellen M. Schmidt²¹, Ian Pan⁵¹, Tamar Sofer^{52,53,54}, Matthias Wuttke⁵⁵, Chloe Sarnowski^{56,281}, Christian Gieger^{57,58,59}, Darryl Nourse⁶⁰, Stella Trompet^{61,62}, Jirong Long⁶³, Meng Sun², Lin Tong⁶⁴, Wei-Min Chen⁶⁵, Meraj Ahmad⁶⁶, Raymond Noordam⁶², Victor J. Y. Lim⁴³, Claudia H. T. Tam^{67,68}, Yoonjung Yoonie Joo^{69,70,282}, Chien-Hsiun Chen⁷¹, Laura M. Raffield³, Cécile Lecoeur^{72,73}, Bram Peter Prins²³, Aude Nicolas⁷⁴, Lisa R. Yanek⁷⁵, Guanjie Chen⁷⁶, Richard A. Jensen⁷⁷, Salman Tajuddin⁷⁸, Edmond K. Kabagambe^{63,283}, Ping An⁷⁹, Anny H. Xiang⁸⁰, Hyeok Sun Choi⁸¹, Brian E. Cade^{20,53}, Jingyi Tan³⁵, Jack Flanagan^{17,48}, Fernando Abaitua^{2,284}, Linda S. Adair⁸², Adebowale Adeyemo⁷⁶, Carlos A. Aguilar-Salinas⁸³, Masato Akiyama^{84,85}, Sonia S. Anand^{36,37,86}, Alain Bertoni⁸⁷, Zheng Bian⁸⁸, Jette Bork-Jensen⁵⁰, Ivan Brandslund^{89,90}, Jennifer A. Brody⁷⁷, Chad M. Brummett⁹¹, Thomas A. Buchanan⁹², Mickaël Canoui^{72,73}, Juliana C. N. Chan^{67,68,93,94}, Li-Ching Chang⁷¹, Miao-Li Chee⁹⁵, Ji Chen^{96,285}, Shyh-Huei Chen⁹⁷, Yuan-Tsong Chen⁷¹, Zhengming Chen^{30,31}, Lee-Ming Chuang^{98,99}, Mary Cushman¹⁰⁰, Swapan K. Das¹⁰¹, H. Janaka de Silva¹⁰², George Dedoussis¹⁰³, Latchezar Dimitrov⁸, Ayo P. Dumaty⁷⁶, Shufa Du^{82,104}, Qing Duan³, Kai-Uwe Eckardt^{105,106}, Leslie S. Emery¹⁰⁷, Daniel S. Evans¹⁰⁸, Michele K. Evans⁷⁸, Krista Fischer⁴⁹, James S. Floyd⁷⁷, Ian Ford¹⁰⁹, Myriam Fornage¹¹⁰, Oscar H. Franco³⁴, Timothy M. Frayling¹¹¹, Barry I. Freedman¹¹², Christian Fuchsberger^{21,113}, Pauline Genter¹¹⁴, Hertzfel C. Gerstein^{36,37,86}, Vilmantas Giedraitis¹¹⁵, Clicerio González-Villalpando¹¹⁶, Maria Elena González-Villalpando¹¹⁶, Mark O. Goodarzi¹¹⁷, Penny Gordon-Larsen^{82,104}, David Gorkin¹¹⁸, Myron Gross¹¹⁹, Yu Guo⁸⁸, Sophie Hacking²³, Sohee Han¹⁶, Andrew T. Hattersley¹²⁰, Christian Herder^{57,121,122}, Annie-Green Howard^{104,123}, Willa Hsueh¹²⁴, Mengna Huang^{51,125}, Wei Huang¹²⁶, Yi-Jen Hung^{127,128}, Mi Yeong Hwang¹⁶, Chii-Min Hwu^{129,130}, Sahoko Ichihara¹³¹, Mohammad Arfan Ikram³⁴, Martin Ingelsson¹¹⁵, Md Tariqul Islam¹³², Masato Isono³³, Hye-Mi Jang¹⁶, Farzana Jasmine⁶⁴, Guozhi Jiang^{67,68}, Jost B. Jonas¹³³, Marit E. Jørgensen^{134,135}, Torben Jørgensen^{136,137,138}, Yoichiro Kamatani^{84,139}, Fouad R. Kandeel¹⁴⁰, Anuradhani Kasturiratne¹⁴¹, Tomohiro Katsuya^{142,143}, Varinderpal Kaur¹⁹, Takahisa Kawaguchi⁴⁶, Jacob M. Keaton^{8,63,286}, Abel N. Kho^{144,145}, Chiea-Chuen Khor¹⁴⁶, Muhammad G. Kibriya⁶⁴, Duk-Hwan Kim¹⁴⁷, Katsuhiko Kohara^{148,287}, Jennifer

Kriebel^{57,58,59}, Florian Kronenberg¹⁴⁹, Johanna Kuusisto¹⁵⁰, Kristi Läll^{49,151}, Leslie A. Lange¹⁵², Myung-Shik Lee^{153,154}, Nanette R. Lee¹⁵⁵, Aaron Leong^{19,156,157}, Liming Li¹⁵⁸, Yun Li³, Ruifang Li-Gao¹⁵⁹, Symen Ligthart³⁴, Cecilia M. Lindgren^{2,160,161}, Allan Linneberg^{136,162}, Ching-Ti Liu⁵⁶, Jianjun Liu^{146,163}, Adam E. Locke^{164,165,288}, Tin Louie¹⁰⁷, Jian'an Luan³⁹, Andrea O. Luk^{67,68}, Xi Luo¹⁶⁶, Jun Lv¹⁵⁸, Valeriya Lyssenko^{167,168}, Vasiliki Mamakou¹⁶⁹, K. Radha Mani^{66,277}, Thomas Meitinger^{170,171,172}, Andres Metspalu⁴⁹, Andrew D. Morris¹⁷³, Girish N. Nadkarni^{32,174,175}, Jerry L. Nadler¹⁷⁶, Michael A. Nalls^{74,177,178}, Uma Nayak⁶⁵, Suraj S. Nongmaithem⁶⁶, Ioanna Ntalla¹⁷⁹, Yukinori Okada^{180,181,182}, Lorena Orozco¹⁸³, Sanjay R. Patel¹⁸⁴, Mark A. Pereira¹⁸⁵, Annette Peters^{57,58,172}, Fraser J. Pirie¹⁸⁶, Bianca Porneala¹⁵⁷, Gauri Prasad^{187,188}, Sebastian Preissl¹¹⁸, Laura J. Rasmussen-Torvik¹⁸⁹, Alexander P. Reiner¹⁹⁰, Michael Roden^{57,121,122}, Rebecca Rohde⁴², Kathryn Roll³⁵, Charumathi Sabanayagam^{95,191,192}, Maïke Sander^{193,194,195}, Kevin Sandow³⁵, Naveed Sattar¹⁹⁶, Sebastian Schönherr¹⁴⁹, Claudia Schurmann^{32,174,197}, Mohammad Shahriar^{64,289}, Jinxiu Shi¹²⁶, Dong Mun Shin¹⁶, Daniel Shriner⁷⁶, Jennifer A. Smith^{45,198}, Wing Yee So^{67,93}, Alena Stan áková¹⁵⁰, Adrienne M. Stilp¹⁰⁷, Konstantin Strauch^{199,200,201}, Ken Suzuki^{17,84,180,202}, Atsushi Takahashi^{84,203}, Kent D. Taylor³⁵, Barbara Thorand^{57,58}, Gudmar Thorleifsson⁴⁷, Unnur Thorsteinsdottir^{47,204}, Brian Tomlinson^{67,205}, Jason M. Torres^{2,290}, Fuu-Jen Tsai²⁰⁶, Jaakko Tuomilehto^{207,208,209,210}, Teresa Tusie-Luna^{211,212}, Miriam S. Udler^{18,19,156}, Adan Valladares-Salgado²¹³, Rob M. van Dam^{43,163}, Jan B. van Klinken^{214,215,216}, Rohit Varma²¹⁷, Marijana Vujkovic²¹⁸, Niels Wacher-Rodarte²¹⁹, Eleanor Wheeler³⁹, Eric A. Whitsel^{42,220}, Ananda R. Wickremasinghe¹⁴¹, Ko Willems van Dijk^{214,215,221}, Daniel R. Witte^{222,223}, Chittaranjan S. Yajnik²²⁴, Ken Yamamoto²²⁵, Toshimasa Yamauchi²⁰², Loïc Yengo²²⁶, Kyunghoon Yoon¹⁶, Canqing Yu¹⁵⁸, Jian-Min Yuan^{227,228}, Salim Yusuf^{36,37,86}, Liang Zhang⁹⁵, Wei Zheng⁶³, FinnGen, eMERGE Consortium, Leslie J. Raffe²²⁹, Michiya Igase²³⁰, Eli Ipp¹¹⁴, Susan Redline^{20,53,231}, Yoon Shin Cho⁸¹, Lars Lind²³², Michael A. Province⁷⁹, Craig L. Hanis²³³, Patricia A. Peyser⁴⁵, Erik Ingelsson^{234,235}, Alan B. Zonderman⁷⁸, Bruce M. Psaty^{77,236,237}, Ya-Xing Wang²³⁸, Charles N. Rotimi⁷⁶, Diane M. Becker⁷⁵, Fumihiko Matsuda⁴⁶, Yongmei Liu^{87,239}, Eleftheria Zeggini^{23,24,240}, Mitsuhiro Yokota²⁴¹, Stephen S. Rich²⁴², Charles Kooperberg¹⁹⁰, James S. Pankow¹⁸⁵, James C. Engert^{243,244}, Yii-Der Ida Chen³⁵, Philippe Froguel^{72,73,245}, James G. Wilson²⁴⁶, Wayne H. H. Sheu^{128,130,247}, Sharon L. R. Kardia⁴⁵, Jer-Yuarn Wu⁷¹, M. Geoffrey Hayes^{69,248,249}, Ronald C. W. Ma^{67,68,93,94}, Tien-Yin Wong^{95,191,192}, Leif Groop^{13,167}, Dennis O. Mook-Kanamori¹⁵⁹, Giriraj R. Chandak⁶⁶, Francis S. Collins²⁵⁰, Dwaipayan Bharadwaj^{187,251}, Guillaume Paré^{37,252}, Michèle M. Sale^{65,277}, Habibul Ahsan⁶⁴, Ayesha A. Motala¹⁸⁶, Xiao-Ou Shu⁶³, Kyong-Soo Park^{22,253,254}, J. Wouter Jukema^{61,255}, Miguel Cruz²¹³, Roberta McKean-Cowdin⁶⁰, Harald Grallert^{57,58,59}, Ching-Yu Cheng^{95,191,192}, Erwin P. Bottinger^{32,174,197}, Abbas Dehghan^{5,34,256}, E-Shyong Tai^{43,163,257}, Josée Dupuis⁵⁶, Norihiro Kato³³, Markku Laakso¹⁵⁰, Anna Köttgen⁵⁵, Woon-Puay Koh^{258,259}, Colin N. A. Palmer²⁶⁰, Simin Liu^{51,125,261}, Goncalo Abecasis²¹, Jaspal S. Kooner^{6,256,262,263}, Ruth J. F. Loos^{32,50,264}, Kari E. North⁴², Christopher A. Haiman⁶⁰, Jose C. Florez^{18,19,156},

Danish Saleheen^{40,265,266}, Torben Hansen⁵⁰, Oluf Pedersen⁵⁰, Reedik Mägi⁴⁹, Claudia Langenberg^{39,267}, Nicholas J. Wareham³⁹, Shiro Maeda^{17,268,269}, Takashi Kadowaki^{202,291}, Juyoung Lee¹⁶, Iona Y. Millwood^{30,31}, Robin G. Walters^{30,31}, Kari Stefansson^{47,204}, Simon R. Myers^{2,270}, Jorge Ferrer^{28,29,271}, Kyle J. Gaulton^{193,194}, James B. Meigs^{18,156,157}, Karen L. Mohlke³, Anna L. Gloyn^{1,2,272,273,†}, Donald W. Bowden^{8,9,274,†}, Jennifer E. Below^{7,†}, John C. Chambers^{5,6,25,256,262,†}, Xueling Sim^{43,†}, Michael Boehnke^{21,†}, Jerome I. Rotter^{35,†}, Mark I. McCarthy^{1,2,272,278,†,‡}, Andrew P. Morris^{2,48,49,275,276,†,‡}

Affiliations

¹Oxford Centre for Diabetes, Endocrinology and Metabolism, Radcliffe Department of Medicine, University of Oxford, Oxford, UK.

²Wellcome Centre for Human Genetics, Nuffield Department of Medicine, University of Oxford, Oxford, UK.

³Department of Genetics, University of North Carolina at Chapel Hill, Chapel Hill, NC, USA.

⁴Department of Epidemiology and Biostatistics, University of Massachusetts-Amherst, Amherst, MA, USA.

⁵Department of Epidemiology and Biostatistics, Imperial College London, London, UK.

⁶Department of Cardiology, Ealing Hospital, London North West Healthcare NHS Trust, London, UK.

⁷Vanderbilt Genetics Institute, Division of Genetic Medicine, Vanderbilt University Medical Center, Nashville, TN, USA.

⁸Center for Genomics and Personalized Medicine Research, Wake Forest School of Medicine, Winston-Salem, NC, USA.

⁹Department of Biochemistry, Wake Forest School of Medicine, Winston-Salem, NC, USA.

¹⁰The Advanced Research Center for Innovations in Next-Generation Medicine (INGEM), Tohoku University, Sendai, Japan.

¹¹Department of Integrative Genomics, Tohoku Medical Megabank Organization, Tohoku University, Sendai, Japan.

¹²Cancer Center, Tohoku University Hospital, Tohoku University, Sendai, Japan.

¹³Institute for Molecular Medicine Finland (FIMM), University of Helsinki, Helsinki, Finland.

¹⁴Genetics Institute, University College London, London, UK.

¹⁵Francis Crick Institute, London, UK.

¹⁶Division of Genome Science, Department of Precision Medicine, National Institute of Health, Cheongju-si, Republic of Korea.

- ¹⁷Laboratory for Genomics of Diabetes and Metabolism, RIKEN Center for Integrative Medical Sciences, Yokohama, Japan.
- ¹⁸Programs in Metabolism and Medical & Population Genetics, Broad Institute of Harvard and MIT, Cambridge, MA, USA.
- ¹⁹Diabetes Unit and Center for Genomic Medicine, Massachusetts General Hospital, Boston, MA, USA.
- ²⁰Harvard Medical School, Boston, MA, USA.
- ²¹Department of Biostatistics and Center for Statistical Genetics, University of Michigan, Ann Arbor, MI, USA.
- ²²Department of Internal Medicine, Seoul National University Hospital, Seoul, South Korea.
- ²³Department of Human Genetics, Wellcome Sanger Institute, Hinxton, UK.
- ²⁴Institute of Translational Genomics, Helmholtz Zentrum München, German Research Center for Environmental Health, Neuherberg, Germany.
- ²⁵Lee Kong Chian School of Medicine, Nanyang Technological University, Singapore, Singapore.
- ²⁶Translational Laboratory in Genetic Medicine (TLGM), Agency for Science, Technology and Research (A*STAR) and National University of Singapore (NUS), Singapore, Singapore.
- ²⁷Biomedical Sciences Graduate Studies Program, University of California San Diego, La Jolla, CA, USA.
- ²⁸Regulatory Genomics and Diabetes, Centre for Genomic Regulation, The Barcelona Institute of Science and Technology, Barcelona, Spain.
- ²⁹Centro de Investigación Biomédica en Red Diabetes y Enfermedades Metabólicas asociadas (CIBERDEM), Madrid, Spain.
- ³⁰Nuffield Department of Population Health, University of Oxford, Oxford, UK.
- ³¹Medical Research Council Population Health Research Unit, University of Oxford, Oxford, UK.
- ³²The Charles Bronfman Institute for Personalized Medicine, Icahn School of Medicine at Mount Sinai, New York, NY, USA.
- ³³Department of Gene Diagnostics and Therapeutics, Research Institute, National Center for Global Health and Medicine, Tokyo, Japan.
- ³⁴Department of Epidemiology, Erasmus University Medical Center, Rotterdam, The Netherlands.
- ³⁵The Institute for Translational Genomics and Population Sciences, Department of Pediatrics, The Lundquist Institute for Biomedical Innovation (formerly Los Angeles

Biomedical Research Institute) at Harbor-UCLA Medical Center, Torrance, CA, USA.

³⁶Department of Medicine, McMaster University, Hamilton, ON, Canada.

³⁷Population Health Research Institute, Hamilton Health Sciences and McMaster University, Hamilton, ON, Canada.

³⁸Public Health Informatics Unit, Department of Integrated Health Sciences, Nagoya University Graduate School of Medicine, Nagoya, Japan.

³⁹MRC Epidemiology Unit, Institute of Metabolic Science, University of Cambridge, Cambridge, UK.

⁴⁰Division of Translational Medicine and Human Genetics, University of Pennsylvania, Philadelphia, PA, USA.

⁴¹Consejo Nacional de Ciencia y Tecnología (CONACYT), Instituto Nacional de Ciencias Médicas y Nutrición Salvador Zubirán, Mexico City, Mexico.

⁴²Department of Epidemiology, Gillings School of Global Public Health, University of North Carolina at Chapel Hill, Chapel Hill, NC, USA.

⁴³Saw Swee Hock School of Public Health, National University of Singapore and National University Health System, Singapore, Singapore.

⁴⁴Department of Anthropology, University of Toronto at Mississauga, Mississauga, ON, Canada.

⁴⁵Department of Epidemiology, School of Public Health, University of Michigan, Ann Arbor, MI, USA.

⁴⁶Center for Genomic Medicine, Kyoto University Graduate School of Medicine, Kyoto, Japan.

⁴⁷deCODE Genetics, Amgen inc., Reykjavik, Iceland.

⁴⁸Department of Health Data Science, University of Liverpool, Liverpool, UK.

⁴⁹Estonian Genome Centre, Institute of Genomics, University of Tartu, Tartu, Estonia.

⁵⁰Novo Nordisk Foundation Center for Basic Metabolic Research, Faculty of Health and Medical Sciences, University of Copenhagen, Copenhagen, Denmark.

⁵¹Department of Epidemiology, Brown University School of Public Health, Providence, RI, USA.

⁵²Department of Biostatistics, Harvard University, Boston, MA, USA.

⁵³Division of Sleep and Circadian Disorders, Brigham and Women's Hospital, Boston, MA, USA.

⁵⁴Department of Medicine, Harvard University, Boston, MA, USA.

⁵⁵Institute of Genetic Epidemiology, Department of Data Driven Medicine, Faculty of Medicine and Medical Center, University of Freiburg, Freiburg, Germany.

⁵⁶Department of Biostatistics, Boston University School of Public Health, Boston, MA, USA.

⁵⁷German Center for Diabetes Research (DZD), Neuherberg, Germany.

⁵⁸Institute of Epidemiology, Helmholtz Zentrum München, German Research Center for Environmental Health, Neuherberg, Germany.

⁵⁹Research Unit of Molecular Epidemiology, Helmholtz Zentrum München, German Research Center for Environmental Health, Neuherberg, Germany.

⁶⁰Department of Population and Public Health Sciences, Keck School of Medicine of USC, Los Angeles, CA, USA.

⁶¹Department of Cardiology, Leiden University Medical Center, Leiden, The Netherlands.

⁶²Section of Gerontology and Geriatrics, Department of Internal Medicine, Leiden University Medical Center, Leiden, The Netherlands.

⁶³Division of Epidemiology, Department of Medicine, Institute for Medicine and Public Health, Vanderbilt Genetics Institute, Vanderbilt University Medical Center, Nashville, TN, USA.

⁶⁴Institute for Population and Precision Health, The University of Chicago, Chicago, IL, USA.

⁶⁵Department of Public Health Sciences and Center for Public Health Genomics, University of Virginia School of Medicine, Charlottesville, VA, USA.

⁶⁶Genomic Research on Complex Diseases (GRC-Group), CSIR-Centre for Cellular and Molecular Biology (CSIR-CCMB), Hyderabad, India.

⁶⁷Department of Medicine and Therapeutics, The Chinese University of Hong Kong, Hong Kong, China.

⁶⁸Chinese University of Hong Kong-Shanghai Jiao Tong University Joint Research Centre in Diabetes Genomics and Precision Medicine, The Chinese University of Hong Kong, Hong Kong, China.

⁶⁹Division of Endocrinology, Metabolism, and Molecular Medicine, Department of Medicine, Northwestern University Feinberg School of Medicine, Chicago, IL, USA.

⁷⁰Department of Health and Biomedical Informatics, Northwestern University Feinberg School of Medicine, Chicago, IL, USA.

⁷¹Institute of Biomedical Sciences, Academia Sinica, Taipei, Taiwan.

⁷²Inserm U1283, CNRS UMR 8199, European Genomic Institute for Diabetes, Institut Pasteur de Lille, Lille, France.

⁷³University of Lille, Lille University Hospital, Lille, France.

- ⁷⁴Laboratory of Neurogenetics, National Institute on Aging, National Institutes of Health, Bethesda, MD, USA.
- ⁷⁵Department of Medicine, Johns Hopkins University School of Medicine, Baltimore, MD, USA.
- ⁷⁶Center for Research on Genomics and Global Health, National Human Genome Research Institute, National Institutes of Health, Bethesda, MD, USA.
- ⁷⁷Cardiovascular Health Research Unit, Department of Medicine, University of Washington, Seattle, WA, USA.
- ⁷⁸Laboratory of Epidemiology and Population Sciences, National Institute on Aging, National Institutes of Health, Baltimore, MD, USA.
- ⁷⁹Division of Statistical Genomics, Washington University School of Medicine, St. Louis, MO, USA.
- ⁸⁰Department of Research and Evaluation, Division of Biostatistics Research, Kaiser Permanente of Southern California, Pasadena, CA, USA.
- ⁸¹Department of Biomedical Science, Hallym University, Chuncheon, South Korea.
- ⁸²Department of Nutrition, Gillings School of Global Public Health, University of North Carolina at Chapel Hill, Chapel Hill, NC, USA.
- ⁸³Unidad de Investigación en Enfermedades Metabólicas and Departamento de Endocrinología y Metabolismo, Instituto Nacional de Ciencias Médicas y Nutrición Salvador Zubirán, Mexico City, Mexico.
- ⁸⁴Laboratory for Statistical and Translational Genetics, RIKEN Center for Integrative Medical Sciences, Yokohama, Japan.
- ⁸⁵Department of Ocular Pathology and Imaging Science, Graduate School of Medical Sciences, Kyushu University, Fukuoka, Japan.
- ⁸⁶Department of Health Research Methods, Evidence, and Impact, McMaster University, Hamilton, ON, Canada.
- ⁸⁷Department of Epidemiology and Prevention, Division of Public Health Sciences, Wake Forest School of Medicine, Winston-Salem, NC, USA.
- ⁸⁸Chinese Academy of Medical Sciences, Beijing, China.
- ⁸⁹Institute of Regional Health Research, University of Southern Denmark, Odense, Denmark.
- ⁹⁰Department of Clinical Biochemistry, Vejle Hospital, Vejle, Denmark.
- ⁹¹Department of Anesthesiology, University of Michigan Medical School, Ann Arbor, MI, USA.
- ⁹²Department of Medicine, Division of Endocrinology and Diabetes, Keck School of Medicine of USC, Los Angeles, CA, USA.

- ⁹³Hong Kong Institute of Diabetes and Obesity, The Chinese University of Hong Kong, Hong Kong, China.
- ⁹⁴Li Ka Shing Institute of Health Sciences, The Chinese University of Hong Kong, Hong Kong, China.
- ⁹⁵Singapore Eye Research Institute, Singapore National Eye Centre, Singapore, Singapore.
- ⁹⁶Wellcome Sanger Institute, Hinxton, UK.
- ⁹⁷Department of Biostatistics and Data Science, Wake Forest School of Medicine, Winston-Salem, NC, USA.
- ⁹⁸Division of Endocrinology and Metabolism, Department of Internal Medicine, National Taiwan University Hospital, Taipei, Taiwan.
- ⁹⁹Institute of Epidemiology and Preventive Medicine, National Taiwan University, Taipei, Taiwan.
- ¹⁰⁰Department of Medicine, University of Vermont, Colchester, VT, USA.
- ¹⁰¹Section on Endocrinology and Metabolism, Department of Internal Medicine, Wake Forest School of Medicine, Winston-Salem, NC, USA.
- ¹⁰²Department of Medicine, Faculty of Medicine, University of Kelaniya, Ragama, Sri Lanka.
- ¹⁰³Department of Nutrition and Dietetics, Harokopio University of Athens, Athens, Greece.
- ¹⁰⁴Carolina Population Center, University of North Carolina at Chapel Hill, Chapel Hill, NC, USA.
- ¹⁰⁵Department of Nephrology and Medical Intensive Care Medicine, Charité Universitätsmedizin Berlin, Berlin, Germany.
- ¹⁰⁶Department of Nephrology and Hypertension, Friedrich-Alexander-Universität Erlangen-Nürnberg, Erlangen, Germany.
- ¹⁰⁷Department of Biostatistics, University of Washington, Seattle, WA, USA.
- ¹⁰⁸California Pacific Medical Center Research Institute, San Francisco, CA, USA.
- ¹⁰⁹Robertson Centre for Biostatistics, University of Glasgow, Glasgow, UK.
- ¹¹⁰Institute of Molecular Medicine, University of Texas Health Science Center at Houston, Houston, TX, USA.
- ¹¹¹Genetics of Complex Traits, University of Exeter Medical School, University of Exeter, Exeter, UK.
- ¹¹²Department of Internal Medicine, Wake Forest School of Medicine, Winston-Salem, NC, USA.

¹¹³Institute for Biomedicine, Eurac Research, Affiliated Institute of the University of Lübeck, Bolzano, Italy.

¹¹⁴Department of Medicine, Division of Endocrinology and Metabolism, Lundquist Research Institute at Harbor-UCLA Medical Center, Torrance, CA, USA.

¹¹⁵Department of Public Health and Caring Sciences, Uppsala University, Uppsala, Sweden.

¹¹⁶Centro de Estudios en Diabetes, Unidad de Investigacion en Diabetes y Riesgo Cardiovascular, Centro de Investigacion en Salud Poblacional, Instituto Nacional de Salud Publica, Mexico City, Mexico.

¹¹⁷Department of Medicine, Division of Endocrinology, Diabetes and Metabolism, Cedars-Sinai Medical Center, Los Angeles, CA, USA.

¹¹⁸Center for Epigenomics, University of California San Diego, La Jolla, CA, USA.

¹¹⁹Department of Laboratory Medicine and Pathology, University of Minnesota, Minneapolis, MN, USA.

¹²⁰University of Exeter Medical School, University of Exeter, Exeter, UK.

¹²¹Institute for Clinical Diabetology, German Diabetes Center, Leibniz Center for Diabetes Research at Heinrich Heine University Düsseldorf, Düsseldorf, Germany.

¹²²Department of Endocrinology and Diabetology, Medical Faculty and University Hospital Düsseldorf, Heinrich Heine University Düsseldorf, Düsseldorf, Germany.

¹²³Department of Biostatistics, Gillings School of Global Public Health, University of North Carolina at Chapel Hill, Chapel Hill, NC, USA.

¹²⁴Department of Internal Medicine, Diabetes and Metabolism Research Center, The Ohio State University Wexner Medical Center, Columbus, OH, USA.

¹²⁵Center for Global Cardiometabolic Health, Brown University, Providence, RI, USA.

¹²⁶Shanghai-MOST Key Laboratory of Health and Disease Genomics, Chinese National Human Genome Center at Shanghai (CHGC) and Shanghai Institute for Biomedical and Pharmaceutical Technologies (SIBPT), Shanghai, China.

¹²⁷Division of Endocrine and Metabolism, Tri-Service General Hospital Songshan Branch, Taipei, Taiwan.

¹²⁸School of Medicine, National Defense Medical Center, Taipei, Taiwan.

¹²⁹Section of Endocrinology and Metabolism, Department of Medicine, Taipei Veterans General Hospital, Taipei, Taiwan.

¹³⁰School of Medicine, National Yang Ming Chiao Tung University, Taipei, Taiwan.

¹³¹Department of Environmental and Preventive Medicine, Jichi Medical University School of Medicine, Shimotsuke, Japan.

¹³²University of Chicago Research Bangladesh, Dhaka, Bangladesh.

- ¹³³Institute of Molecular and Clinical Ophthalmology Basel, Basel, Switzerland.
- ¹³⁴Steno Diabetes Center Copenhagen, Gentofte, Denmark.
- ¹³⁵National Institute of Public Health, Southern Denmark University, Copenhagen, Denmark.
- ¹³⁶Center for Clinical Research and Prevention, Bispebjerg and Frederiksberg Hospital, Frederiksberg, Denmark.
- ¹³⁷Faculty of Health and Medical Sciences, University of Copenhagen, Copenhagen, Denmark.
- ¹³⁸Faculty of Medicine, Aalborg University, Aalborg, Denmark.
- ¹³⁹Laboratory of Complex Trait Genomics, Department of Computational Biology and Medical Sciences, Graduate School of Frontier Sciences, The University of Tokyo, Tokyo, Japan.
- ¹⁴⁰Department of Clinical Diabetes, Endocrinology & Metabolism, Department of Translational Research and Cellular Therapeutics, City of Hope, Duarte, CA, USA.
- ¹⁴¹Department of Public Health, Faculty of Medicine, University of Kelaniya, Ragama, Sri Lanka.
- ¹⁴²Department of Clinical Gene Therapy, Osaka University Graduate School of Medicine, Osaka, Japan.
- ¹⁴³Department of Geriatric and General Medicine, Graduate School of Medicine, Osaka University, Osaka, Japan.
- ¹⁴⁴Division of General Internal Medicine and Geriatrics, Department of Medicine, Northwestern University Feinberg School of Medicine, Chicago, IL, USA.
- ¹⁴⁵Center for Health Information Partnerships, Institute for Public Health and Medicine, Northwestern University Feinberg School of Medicine, Chicago, IL, USA.
- ¹⁴⁶Genome Institute of Singapore, Agency for Science, Technology and Research, Singapore, Singapore.
- ¹⁴⁷Department of Molecular Cell Biology, Sungkyunkwan University School of Medicine, Suwon, South Korea.
- ¹⁴⁸Department of Regional Resource Management, Ehime University Faculty of Collaborative Regional Innovation, Ehime, Japan.
- ¹⁴⁹Institute of Genetic Epidemiology, Department of Genetics and Pharmacology, Medical University of Innsbruck, Innsbruck, Austria.
- ¹⁵⁰Institute of Clinical Medicine, Internal Medicine, University of Eastern Finland and Kuopio University Hospital, Kuopio, Finland.
- ¹⁵¹Institute of Mathematics and Statistics, University of Tartu, Tartu, Estonia.
- ¹⁵²Department of Medicine, University of Colorado Denver, Anschutz Medical Campus, Aurora, CO, USA.

- ¹⁵³Severance Biomedical Science Institute and Department of Internal Medicine, Yonsei University College of Medicine, Seoul, South Korea.
- ¹⁵⁴Department of Medicine, Samsung Medical Center, Sungkyunkwan University School of Medicine, Seoul, South Korea.
- ¹⁵⁵USC-Office of Population Studies Foundation, Inc., University of San Carlos, Cebu City, Philippines.
- ¹⁵⁶Department of Medicine, Harvard Medical School, Boston, MA, USA.
- ¹⁵⁷Division of General Internal Medicine, Massachusetts General Hospital, Boston, MA, USA.
- ¹⁵⁸Department of Epidemiology and Biostatistics, Peking University Health Science Centre, Peking University, Beijing, China.
- ¹⁵⁹Department of Clinical Epidemiology, Leiden University Medical Center, Leiden, The Netherlands.
- ¹⁶⁰Program in Medical & Population Genetics, Broad Institute, Cambridge, MA, USA.
- ¹⁶¹Big Data Institute, Li Ka Shing Centre for Health Information and Discovery, University of Oxford, Oxford, UK.
- ¹⁶²Department of Clinical Medicine, Faculty of Health and Medical Sciences, University of Copenhagen, Copenhagen, Denmark.
- ¹⁶³Department of Medicine, Yong Loo Lin School of Medicine, National University of Singapore and National University Health System, Singapore, Singapore.
- ¹⁶⁴McDonnell Genome Institute, Washington University School of Medicine, St. Louis, MO, USA.
- ¹⁶⁵Department of Medicine, Division of Genomics and Bioinformatics, Washington University School of Medicine, St. Louis, MO, USA.
- ¹⁶⁶Department of Biostatistics and Data Science, University of Texas Health Science Center at Houston, Houston, TX, USA.
- ¹⁶⁷Department of Clinical Sciences, Diabetes and Endocrinology, Lund University Diabetes Centre, Malmö, Sweden.
- ¹⁶⁸Department of Clinical Science, Center for Diabetes Research, University of Bergen, Bergen, Norway.
- ¹⁶⁹Dromokaiteio Psychiatric Hospital, National and Kapodistrian University of Athens, Athens, Greece.
- ¹⁷⁰Institute of Human Genetics, Helmholtz Zentrum München, German Research Center for Environmental Health, Neuherberg, Germany.
- ¹⁷¹Institute of Human Genetics, Technical University of Munich, Munich, Germany.

¹⁷²German Centre for Cardiovascular Research (DZHK), Partner Site Munich Heart Alliance, Munich, Germany.

¹⁷³The Usher Institute to the Population Health Sciences and Informatics, University of Edinburgh, Edinburgh, UK.

¹⁷⁴Digital Health Center, Digital Engineering Faculty of Hasso Plattner Institute and University Potsdam, Potsdam, Germany.

¹⁷⁵The Division of Data Driven and Digital Medicine (D3M), Department of Medicine, Icahn School of Medicine at Mount Sinai, New York, NY, USA.

¹⁷⁶Department of Medicine and Pharmacology, New York Medical College, Valhalla, NY, USA.

¹⁷⁷Data Tecnica International LLC, Glen Echo, MD, USA.

¹⁷⁸Center for Alzheimer's and Related Dementias, National Institutes of Health, Baltimore, MD, USA.

¹⁷⁹William Harvey Research Institute, Barts and The London School of Medicine and Dentistry, Queen Mary University of London, London, UK.

¹⁸⁰Department of Statistical Genetics, Osaka University Graduate School of Medicine, Osaka, Japan.

¹⁸¹Laboratory of Statistical Immunology, Immunology Frontier Research Center (WPI-IFReC), Osaka University, Osaka, Japan.

¹⁸²Laboratory for Systems Genetics, RIKEN Center for Integrative Medical Sciences, Yokohama, Japan.

¹⁸³Instituto Nacional de Medicina Genómica, Mexico City, Mexico.

¹⁸⁴Division of Pulmonary, Allergy, and Critical Care Medicine, Department of Medicine, University of Pittsburgh, Pittsburgh, PA, USA.

¹⁸⁵Division of Epidemiology and Community Health, School of Public Health, University of Minnesota, Minneapolis, MN, USA.

¹⁸⁶Department of Diabetes and Endocrinology, Nelson R Mandela School of Medicine, College of Health Sciences, University of KwaZulu-Natal, Durban, South Africa.

¹⁸⁷Academy of Scientific and Innovative Research, CSIR-Human Resource Development Centre Campus, Ghaziabad, Uttar Pradesh, India.

¹⁸⁸Genomics and Molecular Medicine Unit, CSIR-Institute of Genomics and Integrative Biology, New Delhi, India.

¹⁸⁹Department of Preventive Medicine, Northwestern University Feinberg School of Medicine, Chicago, IL, USA.

¹⁹⁰Fred Hutchinson Cancer Research Center, Seattle, WA, USA.

- ¹⁹¹Ophthalmology and Visual Sciences Academic Clinical Program (Eye ACP), Duke-NUS Medical School, Singapore, Singapore.
- ¹⁹²Department of Ophthalmology, Yong Loo Lin School of Medicine, National University of Singapore and National University Health System, Singapore, Singapore.
- ¹⁹³Department of Pediatrics, Pediatric Diabetes Research Center, University of California San Diego, La Jolla, CA, USA.
- ¹⁹⁴Institute for Genomic Medicine, University of California San Diego, La Jolla, CA, USA.
- ¹⁹⁵Department of Cellular and Molecular Medicine, University of California San Diego, La Jolla, CA, USA.
- ¹⁹⁶Institute of Cardiovascular and Medical Sciences, University of Glasgow, Glasgow, UK.
- ¹⁹⁷Hasso Plattner Institute for Digital Health at Mount Sinai, Icahn School of Medicine at Mount Sinai, New York, NY, USA.
- ¹⁹⁸Survey Research Center, Institute for Social Research, University of Michigan, Ann Arbor, MI, USA.
- ¹⁹⁹Institute of Genetic Epidemiology, Helmholtz Zentrum München, German Research Center for Environmental Health, Neuherberg, Germany.
- ²⁰⁰Chair of Genetic Epidemiology, IBE, Faculty of Medicine, LMU Munich, Munich, Germany.
- ²⁰¹Institute of Medical Biostatistics, Epidemiology and Informatics (IMBEI), University Medical Center, Johannes Gutenberg University, Mainz, Germany.
- ²⁰²Department of Diabetes and Metabolic Diseases, Graduate School of Medicine, The University of Tokyo, Tokyo, Japan.
- ²⁰³Department of Genomic Medicine, National Cerebral and Cardiovascular Center, Osaka, Japan.
- ²⁰⁴Faculty of Medicine, University of Reykjavik, Reykjavik, Iceland.
- ²⁰⁵Faculty of Medicine, Macau University of Science and Technology, Macau, China.
- ²⁰⁶Department of Medical Genetics and Medical Research, China Medical University Hospital, Taichung, Taiwan.
- ²⁰⁷Department of Health, Finnish Institute for Health and Welfare, Helsinki, Finland.
- ²⁰⁸National School of Public Health, Madrid, Spain.
- ²⁰⁹Department of Neuroscience and Preventive Medicine, Danube-University Krems, Krems, Austria.
- ²¹⁰Diabetes Research Group, King Abdulaziz University, Jeddah, Saudi Arabia.

- ²¹¹Unidad de Biología Molecular y Medicina Genómica, Instituto Nacional de Ciencias Médicas y Nutrición Salvador Zubirán, Mexico City, Mexico.
- ²¹²Departamento de Medicina Genómica y Toxicología Ambiental, Instituto de Investigaciones Biomédicas, UNAM, Mexico City, Mexico.
- ²¹³Unidad de Investigación Médica en Bioquímica, Hospital de Especialidades, Centro Médico Nacional Siglo XXI, IMSS, Mexico City, Mexico.
- ²¹⁴Eindhoven Laboratory for Experimental Vascular Medicine, Leiden University Medical Center, Leiden, The Netherlands.
- ²¹⁵Department of Human Genetics, Leiden University Medical Center, Leiden, The Netherlands.
- ²¹⁶Department of Clinical Chemistry, Laboratory of Genetic Metabolic Disease, Amsterdam University Medical Center, Amsterdam, The Netherlands.
- ²¹⁷Southern California Eye Institute, CHA Hollywood Presbyterian Medical Center, Los Angeles, CA, USA.
- ²¹⁸Department of Medicine, University of Pennsylvania Perelman School of Medicine, Philadelphia, PA, USA.
- ²¹⁹Unidad de Investigación Médica en Epidemiología Clínica, Hospital de Especialidades, Centro Médico Nacional Siglo XXI, IMSS, Mexico City, Mexico.
- ²²⁰Department of Medicine, School of Medicine, University of North Carolina at Chapel Hill, Chapel Hill, NC, USA.
- ²²¹Department of Internal Medicine, Division of Endocrinology, Leiden University Medical Center, Leiden, The Netherlands.
- ²²²Department of Public Health, Aarhus University, Aarhus, Denmark.
- ²²³Danish Diabetes Academy, Odense, Denmark.
- ²²⁴Diabetology Research Centre, King Edward Memorial Hospital and Research Centre, Pune, India.
- ²²⁵Department of Medical Biochemistry, Kurume University School of Medicine, Kurume, Japan.
- ²²⁶Institute for Molecular Bioscience, University of Queensland, Brisbane, Australia.
- ²²⁷Division of Cancer Control and Population Sciences, UPMC Hillman Cancer Center, University of Pittsburgh, Pittsburgh, PA, USA.
- ²²⁸Department of Epidemiology, Graduate School of Public Health, University of Pittsburgh, Pittsburgh, PA, USA.
- ²²⁹Department of Pediatrics, Division of Genetic and Genomic Medicine, UCI Irvine School of Medicine, Irvine, CA, USA.
- ²³⁰Department of Anti-aging Medicine, Ehime University Graduate School of Medicine, Ehime, Japan.

- ²³¹Division of Pulmonary, Critical Care, and Sleep Medicine, Beth Israel Deaconess Medical Center, Boston, MA, USA.
- ²³²Department of Medical Sciences, Uppsala University, Uppsala, Sweden.
- ²³³Human Genetics Center, University of Texas Health Science Center at Houston, Houston, TX, USA.
- ²³⁴Department of Medicine, Division of Cardiovascular Medicine, Stanford University School of Medicine, Stanford, CA, USA.
- ²³⁵Department of Medical Sciences, Molecular Epidemiology and Science for Life Laboratory, Uppsala University, Uppsala, Sweden.
- ²³⁶Department of Epidemiology, University of Washington, Seattle, WA, USA.
- ²³⁷Department of Health Services, University of Washington, Seattle, WA, USA.
- ²³⁸Beijing Institute of Ophthalmology, Ophthalmology and Visual Sciences Key Laboratory, Beijing Tongren Hospital, Capital Medical University, Beijing, China.
- ²³⁹Department of Medicine, Division of Cardiology, Duke University School of Medicine, Durham, NC, USA.
- ²⁴⁰Technical University of Munich (TUM) and Klinikum Rechts der Isar, TUM School of Medicine, Munich, Germany.
- ²⁴¹Kurume University School of Medicine, Kurume, Japan.
- ²⁴²Center for Public Health Genomics, University of Virginia School of Medicine, Charlottesville, VA, USA.
- ²⁴³Department of Medicine, McGill University, Montreal, QC, Canada.
- ²⁴⁴Department of Human Genetics, McGill University, Montreal, QC, Canada.
- ²⁴⁵Department of Genomics of Common Disease, School of Public Health, Imperial College London, London, UK.
- ²⁴⁶Department of Physiology and Biophysics, University of Mississippi Medical Center, Jackson, MS, USA.
- ²⁴⁷Division of Endocrinology and Metabolism, Department of Medicine, Taichung Veterans General Hospital, Taichung, Taiwan.
- ²⁴⁸Center for Genetic Medicine, Northwestern University Feinberg School of Medicine, Chicago, IL, USA.
- ²⁴⁹Department of Anthropology, Northwestern University, Evanston, IL, USA.
- ²⁵⁰Center for Precision Health Research, National Human Genome Research Institute, National Institutes of Health, Bethesda, MD, USA.
- ²⁵¹Systems Genomics Laboratory, School of Biotechnology, Jawaharlal Nehru University, New Delhi, India.

- ²⁵²Department of Pathology and Molecular Medicine, McMaster University, Hamilton, ON, Canada.
- ²⁵³Department of Internal Medicine, Seoul National University College of Medicine, Seoul, South Korea.
- ²⁵⁴Department of Molecular Medicine and Biopharmaceutical Sciences, Graduate School of Convergence Science and Technology, Seoul National University, Seoul, South Korea.
- ²⁵⁵Netherlands Heart Institute, Utrecht, The Netherlands.
- ²⁵⁶MRC-PHE Centre for Environment and Health, Imperial College London, London, UK.
- ²⁵⁷Duke-NUS Medical School, Singapore, Singapore.
- ²⁵⁸Singapore Institute for Clinical Sciences, Agency for Science Technology and Research (A*STAR), Singapore, Singapore.
- ²⁵⁹Healthy Longevity Translational Research Programme, Yong Loo Lin School of Medicine, National University of Singapore, Singapore, Singapore.
- ²⁶⁰Pat Macpherson Centre for Pharmacogenetics and Pharmacogenomics, University of Dundee, Dundee, UK.
- ²⁶¹Department of Medicine, Brown University Alpert School of Medicine, Providence, RI, USA.
- ²⁶²Imperial College Healthcare NHS Trust, Imperial College London, London, UK.
- ²⁶³National Heart and Lung Institute, Imperial College London, London, UK.
- ²⁶⁴The Mindich Child Health and Development Institute, Ichan School of Medicine at Mount Sinai, New York, NY, USA.
- ²⁶⁵Department of Biostatistics and Epidemiology, University of Pennsylvania, Philadelphia, PA, USA.
- ²⁶⁶Center for Non-Communicable Diseases, Karachi, Pakistan.
- ²⁶⁷Computational Medicine, Berlin Institute of Health at Charité Universitätsmedizin, Berlin, Germany.
- ²⁶⁸Department of Advanced Genomic and Laboratory Medicine, Graduate School of Medicine, University of the Ryukyus, Okinawa, Japan.
- ²⁶⁹Division of Clinical Laboratory and Blood Transfusion, University of the Ryukyus Hospital, Okinawa, Japan.
- ²⁷⁰Department of Statistics, University of Oxford, Oxford, UK.
- ²⁷¹Section of Genetics and Genomics, Department of Metabolism, Digestion and Reproduction, Imperial College London, London, UK.

²⁷²Oxford NIHR Biomedical Research Centre, Churchill Hospital, Oxford University Hospitals NHS Foundation Trust, Oxford, UK.

²⁷³Division of Endocrinology, Department of Pediatrics, Stanford School of Medicine, Stanford University, Stanford, CA, USA.

²⁷⁴Center for Diabetes Research, Wake Forest School of Medicine, Winston-Salem, NC, USA.

²⁷⁵Centre for Genetics and Genomics Versus Arthritis, Centre for Musculoskeletal Research, Division of Musculoskeletal and Dermatological Sciences, University of Manchester, Manchester, UK.

²⁷⁶NIHR Manchester Biomedical Research Centre, Manchester University NHS Foundation Trust, Manchester, UK.

²⁷⁷Deceased.

²⁷⁸Present address: Genentech, South San Francisco, CA, USA.

²⁷⁹Present address: Internal Medicine Research Unit, Pfizer Worldwide Research, Cambridge, MA, USA.

²⁸⁰Present address: Departamento de Medicina Genómica y Toxicología Ambiental, Instituto de Investigaciones Biomédicas, UNAM, Ciudad de Mexico, Mexico.

²⁸¹Present address: The University of Texas Health Science Center at Houston, School of Public Health, Department of Epidemiology, Human Genetics, and Environmental Sciences, Houston, TX, USA.

²⁸²Present address: Institute of Data Science, Korea University, Seoul, South Korea.

²⁸³Present address: Division of Academics, Ochsner Health, New Orleans, LA, USA.

²⁸⁴Present address: Vertex Pharmaceuticals Ltd, Oxford, UK.

²⁸⁵Present address: Exeter Centre of Excellence in Diabetes (ExCEeD), Exeter Medical School, University of Exeter, Exeter, UK.

²⁸⁶Present address: Center for Precision Health Research, National Human Genome Research Institute, National Institutes of Health, Bethesda, MD, USA.

²⁸⁷Present address: Ibusuki Kozenkai Hospital, Ibusuki, Japan.

²⁸⁸Present address: Regeneron Genetics Center, Tarrytown, NY, USA

²⁸⁹Present address: Institute for Population and Precision Health (IPPH), Biological Sciences Division, The University of Chicago, Chicago, IL, USA.

²⁹⁰Present address: Clinical Trial Service Unit and Epidemiological Studies Unit, Nuffield Department of Population Health, University of Oxford, Oxford, UK.

²⁹¹Present address: Toranomom Hospital, Tokyo, Japan.

ACKNOWLEDGEMENTS

A complete list acknowledgments and funding appears in the Supplementary Note. This research was funded in whole, or in part, by the Wellcome Trust (grant numbers 064890, 072960, 083948, 084723, 085475, 086113, 088158, 090367, 090532, 095101, 098017, 098051, 098381, 098395, 101033, 101630, 104085, 106130, 200186, 200837, 202922, 203141, 206194, 212259, 212284, 212946, 220457). For the purpose of Open Access, the authors have applied a CC-BY public copyright licence to any Author Accepted Manuscript version arising from this submission.

Data availability statement.

Association summary statistics from the multi-ancestry meta-analysis and annotation-informed fine-mapping are available through the AMP-T2D Knowledge Portal (<http://www.type2diabetesgenetics.org/>) and the DIAGRAM Consortium Data Download website (<http://diagram-consortium.org/downloads.html>).

Appendix

CONSORTIA

FinnGen

Sina Rüeger¹⁴ and Pietro della Briotta Parolo¹⁴

Contributors to FinnGen are listed in the Supplementary Note.

eMERGE Consortium

Yoonjung Yoonie Joo^{68,69}, Abel N. Kho^{144,145}, and M. Geoffrey Hayes^{68,247,248}

Contributors to the eMERGE Consortium are listed in the Supplementary Note.

REFERENCES

1. NCD Risk Factor Collaboration. Worldwide trends in diabetes since 1980: a pooled analysis of 751 population-based studies with 4.4 million participants. *Lancet* 387, 1513–1530 (2016). [PubMed: 27061677]
2. GBD 2015 Disease and Injury Incidence and Prevalence Collaborators. Global, regional, and national incidence, prevalence, and years lived with disability for 310 diseases and injuries, 1990–2015: a systematic analysis for the Global Burden of Disease Study 2015. *Lancet* 388, 1545–1602 (2016). [PubMed: 27733282]
3. Voight BF et al. Twelve type 2 diabetes susceptibility loci identified through large-scale association analysis. *Nat. Genet* 42, 579–589 (2010). [PubMed: 20581827]
4. Morris AP et al. Large-scale association analysis provides insights into the genetic architecture and pathophysiology of type 2 diabetes. *Nat. Genet* 44, 981–990 (2012). [PubMed: 22885922]
5. Scott RA et al. An expanded genome-wide association study of type 2 diabetes in Europeans. *Diabetes* 66, 2888–2902 (2017). [PubMed: 28566273]
6. Mahajan A et al. Fine-mapping type 2 diabetes loci to single-variant resolution using high-density imputation and islet-specific epigenome maps. *Nat. Genet* 50, 1505–1513 (2018). [PubMed: 30297969]
7. Moltke I et al. A common Greenlandic TBC1D4 variant confers muscle insulin resistance and type 2 diabetes. *Nature* 512, 190–193 (2014). [PubMed: 25043022]
8. Martin AR et al. Human demographic history impacts genetic risk prediction across diverse populations. *Am. J. Hum. Genet* 100, 635–649 (2017). [PubMed: 28366442]

9. Suzuki K et al. Identification of 28 new susceptibility loci for type 2 diabetes in the Japanese population. *Nat. Genet* 51, 379–386 (2019). [PubMed: 30718926]
10. Spracklen CN et al. Identification of type 2 diabetes loci in 433,540 East Asian individuals. *Nature* 582, 240–245 (2020). [PubMed: 32499647]
11. Vujkovic M et al. Discovery of 318 new risk loci for type 2 diabetes and related vascular outcomes among 1.4 million participants in a multi-ancestry meta-analysis. *Nat. Genet* 52, 680–691 (2020). [PubMed: 32541925]
12. The 1000 Genomes Project Consortium. An integrated map of genetic variation from 1,092 human genomes. *Nature* 491, 56–65 (2012). [PubMed: 23128226]
13. The 1000 Genomes Project Consortium. A global reference for human genetic variation. *Nature* 526, 68–74 (2015). [PubMed: 26432245]
14. McCarthy S et al. A reference panel of 64,976 haplotypes for genotype imputation. *Nat. Genet* 48, 1279–1283 (2016). [PubMed: 27548312]
15. Mägi R et al. Trans-ethnic meta-regression of genome-wide association studies accounting for ancestry increases power for discovery and improves fine-mapping resolution. *Hum. Mol. Genet* 26, 3639–3650 (2017). [PubMed: 28911207]
16. Chen M-H et al. Trans-ethnic and ancestry-specific blood-cell genetics in 746,667 individuals from 5 global populations. *Cell* 182, 1198–1213 (2020). [PubMed: 32888493]
17. Mahajan A et al. Refining the accuracy of validated target identification through coding variant fine-mapping in type 2 diabetes. *Nat. Genet* 50, 559–571 (2018). [PubMed: 29632382]
18. Varshney A et al. Genetic regulatory signatures underlying islet gene expression and type 2 diabetes. *Proc. Natl. Acad. Sci. U. S. A* 114, 2301–2306 (2017). [PubMed: 28193859]
19. Zhao F et al. Nodal induces apoptosis through activation of the ALK7 signaling pathway in pancreatic INS-1 β -cells. *Am. J. Physiol. Endocrinol. Metab* 303, E132–43 (2012). [PubMed: 22550067]
20. Emdin CA et al. DNA sequence variation in ACVR1C encoding the activin receptor-like kinase 7 influences body fat distribution and protects against type 2 diabetes. *Diabetes* 68, 226–234 (2019). [PubMed: 30389748]
21. Sun BB et al. Genomic atlas of the human plasma proteome. *Nature* 558, 73–79 (2018). [PubMed: 29875488]
22. Consortium GTEx. Genetic effects on gene expression across human tissues. *Nature* 550, 204–213 (2017). [PubMed: 29022597]
23. Vinuela A et al. Genetic variant effects on gene expression in human pancreatic islets and their implications for T2D. *Nat. Commun* 11, 4912 (2020). [PubMed: 32999275]
24. Giambartolomei C et al. Bayesian test for colocalization between pairs of genetic association studies using summary statistics. *PLoS Genet*. 10, e1004383 (2014). [PubMed: 24830394]
25. van de Bunt M et al. Transcript expression data from human islets links regulatory signals from genome-wide association studies for type 2 diabetes and glycemic traits to their downstream effectors. *PLoS Genet*. 11, e1005694 (2015). [PubMed: 26624892]
26. Roman TS et al. A type 2 diabetes-associated functional regulatory variant in a pancreatic islet enhancer at the ADCY5 locus. *Diabetes* 66, 2521–2530 (2017). [PubMed: 28684635]
27. Carrat GR et al. Decreased STARD10 expression is associated with defective insulin secretion in humans and mice. *Am. J. Hum. Genet* 100, 238–256 (2017). [PubMed: 28132686]
28. Small KS et al. Regulatory variants at KLF14 influence type 2 diabetes risk via a female-specific effect on adipocyte size and body composition. *Nat. Genet* 50, 572–580 (2018). [PubMed: 29632379]
29. Thurner M et al. Integration of human pancreatic islet genomic data refines regulatory mechanisms at type 2 diabetes susceptibility loci. *Elife* 7, e31977 (2018). [PubMed: 29412141]
30. Pan DZ et al. Integration of human adipocyte chromosomal interactions with adipose gene expression prioritizes obesity-related genes from GWAS. *Nat. Commun* 9, 1512 (2018). [PubMed: 29666371]

31. Miguel-Escalada I et al. Human pancreatic islet three-dimensional chromatin architecture provides insights into the genetics of type 2 diabetes. *Nat. Genet* 51, 1137–1148 (2019). [PubMed: 31253982]
32. Chesi A et al. Genome-scale Capture C promoter interactions implicate effector genes at GWAS loci for bone mineral density. *Nat. Commun* 10, 1260 (2019). [PubMed: 30890710]
33. Chiou J et al. Single-cell chromatin accessibility reveals pancreatic islet cell type- and state-specific regulatory programs of diabetes risk. *Nat. Genet* 53, 455–466 (2021). [PubMed: 33795864]
34. Esteghamat F et al. CELA2A mutations predispose to early-onset atherosclerosis and metabolic syndrome and affect plasma insulin and platelet activation. *Nat. Genet* 51, 1233–1243 (2019). [PubMed: 31358993]
35. Ng NHJ et al. Tissue-specific alteration of metabolic pathways influences glycemic regulation. Preprint at <https://www.biorxiv.org/content/10.1101/790618v1> (2019).
36. Gloyd AL Exocrine or endocrine? A circulating pancreatic elastase that regulates glucose homeostasis. *Nat. Metab* 1, 853–855 (2019). [PubMed: 32694741]
37. Wesolowska-Andersen A et al. Deep learning models predict regulatory variants in pancreatic islets and refine type 2 diabetes association signals. *Elife* 9, e51503 (2020). [PubMed: 31985400]
38. Martin AR et al. Clinical use of current polygenic risk scores may exacerbate health disparities. *Nat. Genet* 51, 584–591 (2019). [PubMed: 30926966]
39. Mars N et al. Polygenic and clinical risk scores and their impact on age at onset and prediction of cardiometabolic diseases and common cancers. *Nat. Med* 26, 549–557 (2020). [PubMed: 32273609]
40. Ayub Q et al. Revisiting the thrifty gene hypothesis via 65 loci associated with susceptibility to type 2 diabetes. *Am. J. Hum. Genet* 94, 176–185 (2014). [PubMed: 24412096]
41. Neel JV Diabetes mellitus: a “thrifty” genotype rendered detrimental by “progress”? *Am. J. Hum. Genet* 14, 353–362 (1962). [PubMed: 13937884]
42. Speidel L, Forest M, Shi S & Myers SR A method for genome-wide genealogy estimation for thousands of samples. *Nat. Genet* 51, 1321–1329 (2019). [PubMed: 31477933]
43. Bycroft C et al. The UK Biobank resource with deep phenotyping and genomic data. *Nature* 562, 203–209 (2018). [PubMed: 30305743]
44. Chen R et al. Type 2 diabetes risk alleles demonstrate extreme directional differentiation among human populations, compared to other diseases. *PLoS Genet.* 8, e1002621 (2012). [PubMed: 22511877]
45. Lewis ACF et al. Getting genetic ancestry right for science and society. Preprint at <https://arxiv.org/abs/2110.05987v2> (2021).
46. Kanai M et al. Insights from complex trait fine-mapping across diverse populations. Preprint at <https://www.medrxiv.org/content/10.1101/2021.09.03.21262975v1> (2021).
47. Taliun D et al. Sequencing of 53,831 diverse genomes from the NHLBI TOPMed Program. *Nature* 590, 290–299 (2021). [PubMed: 33568819]
48. Jónsson H et al. Whole genome characterization of sequence diversity of 15,220 Icelanders. *Sci. Data* 4, 170115 (2017). [PubMed: 28933420]
49. Mitt M et al. Improved imputation accuracy of rare and low-frequency variants using population-specific high-coverage WGS-based imputation reference panel. *Eur. J. Hum. Genet* 25, 869–876 (2017). [PubMed: 28401899]
50. Moon S et al. The Korea Biobank Array: design and identification of coding variants associated with blood biochemical traits. *Sci. Rep* 9, 1382 (2019). [PubMed: 30718733]
51. Cook JP, Mahajan A & Morris AP Guidance for the utility of linear models in meta-analysis of genetic association studies of binary phenotypes. *Eur. J. Hum. Genet* 25, 240–245 (2016). [PubMed: 27848946]
52. Devlin B & Roeder K Genomic control for association studies. *Biometrics* 55, 997–1004 (1999). [PubMed: 11315092]
53. Gurdasani D, Barroso I, Zeggini E & Sandhu MS Genomics of disease risk in globally diverse populations. *Nat. Rev. Genet* 20, 520–535 (2019). [PubMed: 31235872]

54. Willer CJ, Li Y & Abecasis GR METAL: fast and efficient meta-analysis of genome-wide association scans. *Bioinformatics* 26, 2190–2191 (2010). [PubMed: 20616382]
55. Han B & Eskin E Random-effects model aimed at discovering associations in meta-analysis of genome-wide association studies. *Am. J. Hum. Genet* 88, 586–598 (2011). [PubMed: 21565292]
56. Purcell S et al. PLINK: a tool set for whole-genome association and population-based linkage analyses. *Am. J. Hum. Genet* 81, 559–575 (2007). [PubMed: 17701901]
57. Sobota RS et al. Addressing population-specific multiple testing burdens in genetic association studies. *Ann. Hum. Genet* 79, 136–147 (2015). [PubMed: 25644736]
58. Yang J et al. Conditional and joint multiple-SNP analysis of GWAS summary statistics identifies additional variants influencing complex traits. *Nat. Genet* 44, 369–375 (2012). [PubMed: 22426310]
59. Kass RE & Raftery AE (1995). Bayes factors. *J. Am. Stat. Assoc* 90, 773–795 (1995).
60. Maller JB et al. Bayesian refinement of association signals for 14 loci in 3 common diseases. *Nat. Genet* 44, 1294–1301 (2012). [PubMed: 23104008]
61. Harrow J et al. GENCODE: the reference human genome annotation for The ENCODE Project. *Genome Res.* 22, 1760–1774 (2012). [PubMed: 22955987]
62. ENCODE Project Consortium. An integrated encyclopedia of DNA elements in the human genome. *Nature* 489, 57–74 (2012). [PubMed: 22955616]
63. Pasquali L et al. Pancreatic islet enhancer clusters enriched in type 2 diabetes risk-associated variants. *Nat. Genet* 46, 136–143 (2014). [PubMed: 24413736]
64. Pickrell J Joint analysis of functional genomic data and genome-wide association studies of 18 human traits. *Am. J. Hum. Genet* 94, 559–573 (2014). [PubMed: 24702953]
65. Wakefield JA Bayesian measure of the probability of false discovery in genetic epidemiology studies. *Am. J. Hum. Genet* 81, 208–227 (2007). [PubMed: 17668372]
66. Ravassard P et al. A genetically engineered human pancreatic β cell line exhibiting glucose-inducible insulin secretion. *J. Clin. Invest* 121, 3589–3597 (2011). [PubMed: 21865645]

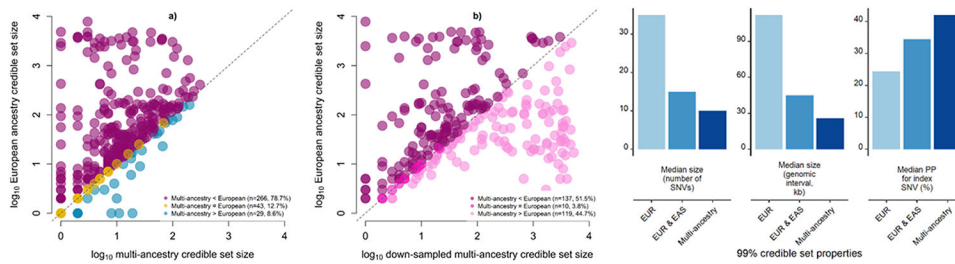


Figure 1 | Comparison of fine-mapping resolution for distinct association signals for T2D obtained from ancestry-specific meta-analysis and multi-ancestry meta-regression.

a. Each point corresponds to a distinct association signal, plotted according to the \log_{10} credible set size in the multi-ancestry meta-regression on the x-axis and the \log_{10} credible set size in the European ancestry meta-analysis on the y-axis. The 266 (78.7%) signals above the dashed $y = x$ line were more precisely fine-mapped in the multi-ancestry meta-regression. **b.** We “down-sampled” the multi-ancestry meta-regression to the effective sample size of the European ancestry-specific meta-analysis. Each point corresponds to one of the 266 signals that were more precisely fine-mapped in the multi-ancestry meta-regression. The 137 (51.5%) signals above the dashed $y = x$ line were more precisely fine-mapped in “down-sampled” multi-ancestry meta-regression than the equivalent sized European ancestry-specific meta-analysis. **c.** Properties of 99% credible sets of variants driving each distinct association signal in European ancestry-specific meta-analysis, combined East Asian and European ancestry meta-analysis, and multi-ancestry meta-regression. The inclusion of the most under-represented ancestry groups (African, Hispanic and South Asian) in the multi-ancestry meta-regression reduced the median size of 99% credible sets and increased the median posterior probability ascribed to index SNVs.

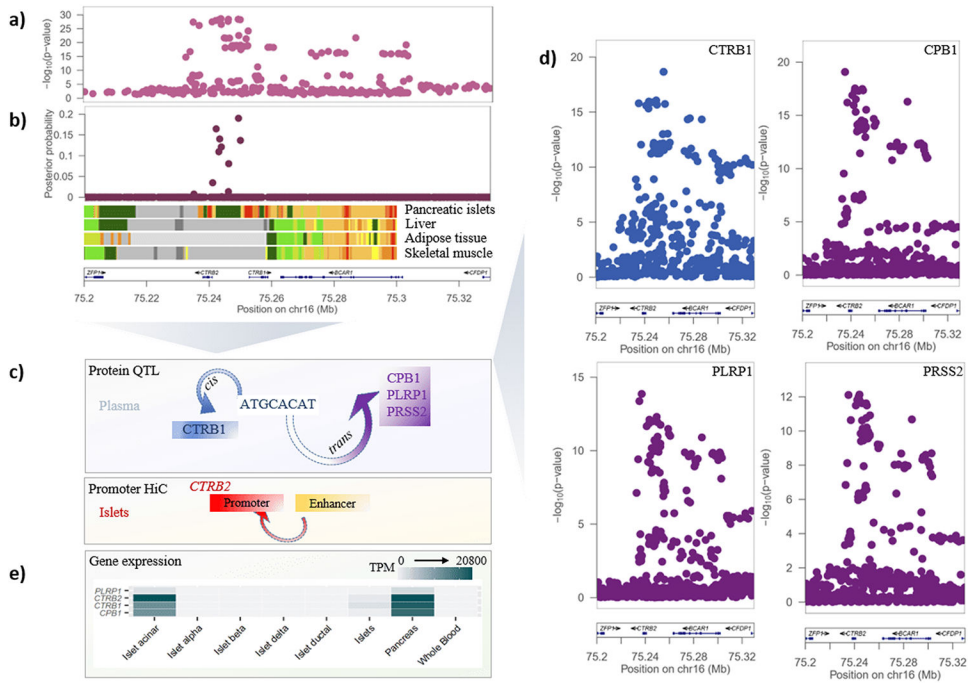


Figure 2 | T2D association signal at the *BCAR1* locus colocalizes with multiple circulating plasma pQTLs.

a, Signal plot for T2D association from multi-ancestry meta-regression of 180,834 cases and 1,159,055 controls of diverse ancestry. Each point represents an SNV, plotted with their P -value (on a \log_{10} scale) as a function of genomic position (NCBI build 37). Gene annotations are taken from the University of California Santa Cruz genome browser. Recombination rates are estimated from the Phase II HapMap. **b**, Fine-mapping of T2D association signal from multi-ancestry meta-regression. Each point represents an SNV plotted with their posterior probability of driving T2D association as a function of genomic position (NCBI build 37). Chromatin states are presented for four diabetes-relevant tissues: active TSS (red), flanking active TSS (orange red), strong transcription (green), weak transcription (dark green), genic enhancers (green yellow), active enhancer (orange), weak enhancer (yellow), bivalent/poised TSS (Indian red), flanking bivalent TSS/enhancer (dark salmon), repressed polycomb (silver), weak repressed polycomb (Gainsboro), quiescent/low (white). **c**, Schematic presentation of the single *cis*- and multiple *trans*- effects mediated by the *BCAR1* locus on plasma proteins and the islet chromatin loop between islet enhancer and promoter elements near *CTRB2*. **d**, Signal plots for four circulating plasma proteins that colocalize with the T2D association in 3,301 European ancestry participants from the INTERVAL study. Each point represents an SNV, plotted with their P -value (on a \log_{10} scale) as a function of genomic position (NCBI build 37). **e**, Expression of genes (transcripts per million, TPM) encoding colocalized proteins in islets, pancreas and whole blood.

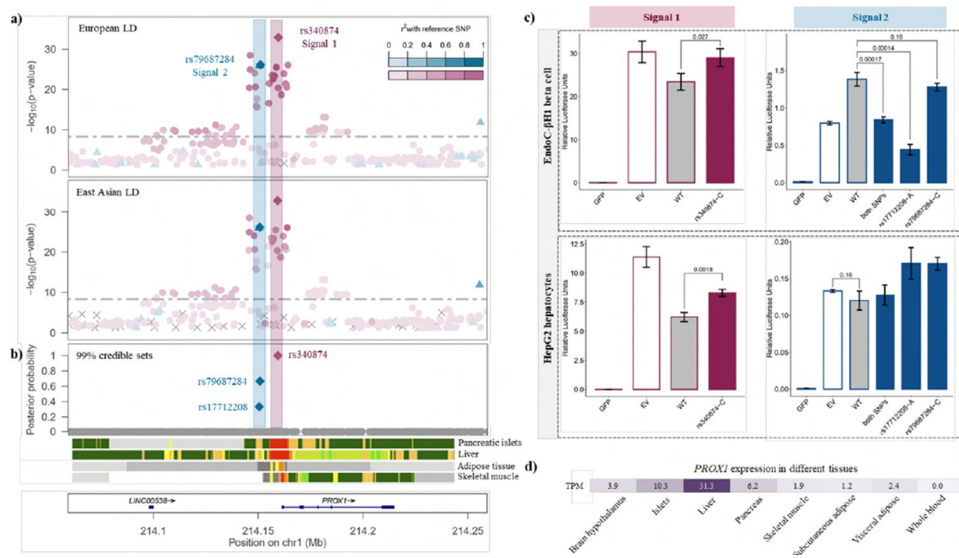


Figure 3 | Defining causal molecular mechanisms at the *PROX1* locus.

a, Signal plot for two distinct T2D associations from multi-ancestry meta-regression of 180,834 cases and 1,159,055 controls of diverse ancestry. Each point represents an SNV, plotted with their P -value (on a $-\log_{10}$ scale) as a function of genomic position (NCBI build 37). Index SNVs are represented by the blue and purple diamonds. All other SNVs are colored according to the LD with the index SNVs in European and East Asian ancestry populations. Gene annotations are taken from the University of California Santa Cruz genome browser. **b**, Fine-mapping of T2D association signals from multi-ancestry meta-regression. Each point represents a SNV plotted with their posterior probability of driving each distinct T2D association as a function of genomic position (NCBI build 37). The 99% credible sets for the two signals are highlighted by the purple and blue diamonds. Chromatin states are presented for four diabetes-relevant tissues: active TSS (red), flanking active TSS (orange red), strong transcription (green), weak transcription (dark green), genic enhancers (green yellow), active enhancer (orange), weak enhancer (yellow), bivalent/poised TSS (Indian red), flanking bivalent TSS/enhancer (dark salmon), repressed polycomb (silver), weak repressed polycomb (Gainsboro), quiescent/low (white). **c**, Transcriptional activity of the 99 credible set variants at the two T2D association signals in human HepG2 hepatocytes and EndoC- β H1 beta cell models obtained from *in vitro* reporter assays. Biological replicates: $n = 3$. Technical replicates: $n = 3$. WT, wild-type (non-risk allele/haplotype); GFP, green fluorescent protein (negative control); EV, empty vector (baseline). Height of bar represents mean. Error bars represent standard error of the mean. Differences in luciferase activity between groups were tested using two-tailed two-sample t -tests, where $P < 0.05$ was considered statistically significant. **d**, Expression of *PROX1* (transcripts per million, TPM) across a range of diabetes-relevant tissues.



Figure 4 |. Transferability of multi-ancestry and ancestry-specific GRS into GWAS across diverse population groups.

Each GRS was constructed using lead SNVs attaining genome-wide significance ($P < 5 \times 10^{-9}$ for multi-ancestry GRS and $P < 5 \times 10^{-8}$ for ancestry-specific GRS). For the multi-ancestry GRS, population-specific allelic effects on T2D were estimated from the meta-regression to generate different GRS weights for each test GWAS. For each ancestry-specific GRS, weights were generated from allelic effect estimates obtained from fixed-effects meta-analysis. **a**, The trait variance explained (pseudo R^2) by each GRS was assessed in two test GWAS from each ancestry group. **b**, The multi-ancestry GRS out-performed ancestry-specific GRS into all test GWAS, reflecting the shared genetic contribution to T2D across diverse populations, despite differing allele frequencies and LD patterns.

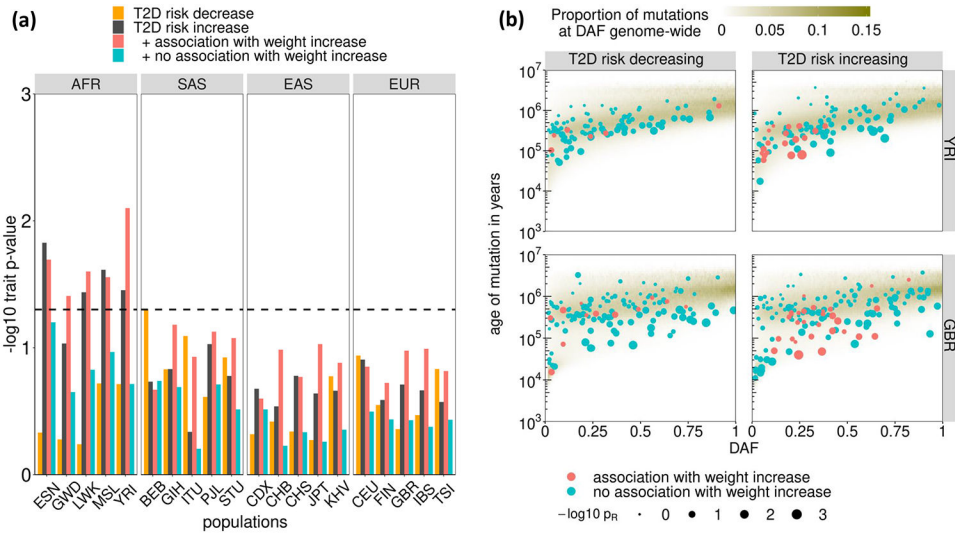


Figure 5 | Positive selection acting on T2D index SNVs.

a, Evidence of selection from Relate towards increased T2D risk is restricted to African ancestry populations and is explained by those SNVs that are associated with increased weight. **b**, T2D risk alleles that are associated with increased weight are particularly young for their derived allele frequency (DAF). Population abbreviations (sample sizes): ESN (98), Esan in Nigeria; GWD (112), Gambian in Western Divisions of the Gambia; LWK (98), Luhya in Webuye, Kenya; MSL (84), Mende in Sierra Leone; YRI (107), Yoruba in Ibadan, Nigeria; BEB (85), Bengali in Bangladesh; GIH (102), Gujarati Indian from Houston, Texas; ITU (101), Indian Telegu from the UK; PJI (95), Punjabi from Lahore, Pakistan; STU (101), Sri Lankan Tamil from the UK; CDX (92), Chinese Dai in Xishuangbanna, China; CHB (102), Han Chinese in Beijing, China; CHS (104), Southern Han Chinese; JPT (103), Japanese in Tokyo, Japan; KHV (98), Kinh in Ho Chi Min City, Vietnam; CEU (98), Utah residents with Northern and Western European ancestry; FIN (98), Finnish in Finland; GBR (90), British in England and Scotland; IBS (106), Iberian population in Spain; TSI (106), Toscani in Italy.